Finite Element Analysis of Tendon's Collagen Network in Three Dimensions

By

DOROTHEA POLITIS

A thesis submitted to the

Graduate School-New Brunswick

Rutgers, The State University of New Jersey and

The Graduate School of Biomedical Sciences

University of Medicine and Dentistry of New Jersey

in partial fulfillment of the requirements

for the degree of

Master of Science

Graduate Program in Biomedical Engineering

written under the direction of

Dr. Frederick H. Silver

and approved by

_____

_____

_____

_____

New Brunswick, New Jersey

January, 2014

ABSTRACT OF THE THESIS

Finite Element Analysis of Tendon's Collagen Network in Three Dimensions

By DOROTHEA POLITIS

Thesis Director

Dr. Frederick Silver

One of the most vital parts of the human body is the tendon. The main focus of this research is the development of a solid finite element model in three dimensions for the tendon's collagenous network. Most of the previous studies use simplified approaches in two or three dimensions without including tendon's essential network. A multi-level approach at the lower levels of hierarchy, such as the microfibrils, will be beneficial in understanding tissue function. Cross-links operate significantly at the fibril level. Thus, determining their influence on mechanical function at this level is important to appreciate the ways in which the macroscopic level is affected.

Analytical finite element models in 3D that describe the mechanical behavior of the complex collagen network and predict stresses in its individual components are still lacking. This study develops a 3D model, based on Orgel's microfibril structure, consisting of the mineral and collagen D-bands, as well as their intermolecular crosslinks. This structure includes multiple molecules that are aligned in parallel and form the collagen fibril with a D-band repetition every 67nm, while they are organized in a quasi-hexagonal pattern in the cross section. In this study the created collagen matrix model is subjected to tensile loads in order to estimate the stress-strain behavior and the Young's Modulus in the elastic regime. With the use of finite element analysis this model requires less computational time than using a Molecular Dynamics Software. Furthermore, parametric analysis of the mineralization and hydration phase under tension is investigated. Results report total elastic modulus of various parametrical models that agree well with previously reported experimental and Steer Molecular Dynamics studies.

To my brother in the army,
my mother in Greece,
my father in Saudi Arabia,
and all my friends and family in Greece and U.S.
for their support.

ACKNOWLEDGMENTS

I would like to thank for their help and support,

- My advisor for his insight Dr. Frederick Silver*, Rutgers-UMDNJ, Biomedical Engineering department,*
- Dr. Ellis Harold Dill for his guidance in FEA, *Rutgers, Mechanical and Aerospace Engineering department,*
- My mentor Dr. Jim Pennline, *at N.A.S.A Glenn Research Center,*
- Dr. Noshir A. Langrana for his participation in the committee, *Rutgers, Biomedical Engineering department,*
- Dr. Ronke Olabisi, for her participation in the committee, *Rutgers, Biomedical Engineering department,*

And all of my professors and directors in the Biomedical Engineering department of Rutgers University.

TABLE OF CONTENTS

CHAPTER 1

INTRODUCTION

1.1 Purpose

Distribution of the interacting forces-displacements among the components of the tendon's network is of prime importance to better understand force transmission, energy storage and dissipation in tendons. This can be achieved by detailed formation of the structure involved in each level of hierarchy. In addition, the knowledge of such forces-displacements is fundamental for various implants designs, muscular strengthening and rehabilitation. Apart from the experimental studies in all macroscopic hierarchical levels of tendon, mathematical and computational models of microfibril structure have been developed to predict the approximated biomechanical behavior of individual fibrous tissue. Analytical methods are not convenient due to the complexity of the structures and the perplexity of solving many high order differential equations. Since 1990, the development of feasible technological methods and tools made numerical methods possible and led to the introduction of finite element analysis (FEA), a highly popular tool for the modeling of problems in biomechanics. With this method we can establish the stress behavior that is influenced from the model's material properties and the geometrical features.

1.2 Tendon Structure

Tendon is responsible for the transmission of forces and connection of muscle to bone. It is a high order extracellular matrix [7]. Tendons mainly contain cells such as fibroblasts, endothelial cells, chondrocytes, proteins such as collagen type I and small amounts of

type III and IV collagens. Proteoglycans are also found in tendons, mainly decorin, water and hyaluronan. They are associated with the alignment and the geometry of the collagen. Decorin is responsible for fibrillogenesis and potential abnormalities of the shape of collagen [1, 7]. Also, decorin can maintain a healthy and normal connective tissue and extracellular matrix. The main structures of tendons are the fascicles which are formed by fibril bundles. Collagen molecules form the collagen fibrils which assemble into these fiber bundles, and are usually parallel to the tendon's long axis [Fig. 1]. The collagen fiber has an average diameter of 3-5μm, while the fibril is 0.1μm and the molecule less than 1.5nm. Other studies report that the various hierarchical diameters range from 2nm for molecules, over 200nm for fibrils, 2μm for fibers and from 200μm fascicles to tendons of 10mm [25]. Collagen fibril diameters in turkey tendon range from 25 to 500nm. These molecules inside the fibril show a slight angle no more than 5^{o} [7]. Collagen fibrils, also, branch form larger tendons and increase in size as they develop [10].

Many types of tendons in human and mammals form various patterns. The shape of tendons varies from cylindrical to flat shape [7]. Short but thick tendons appear in muscles that produce powerful resistant forces, such as quadriceps, while muscles that are associated with gentle movements have long and thin tendons. Inside the fibers the collagen fibrils are arranged longitudinally, horizontally or transversally to fibers' length [7]. Mechanical properties in tendon are associated with the diameter of collagen fibrils. Small diameter fibrils are elastic and creep resistant while larger diameters fibrils are stronger because of their increased density of crosslinks. Collagen fibril diameter tends to

decrease with age. However, the diameter has less influence on the elastic modulus and tensile strength than the actual length of the fibrils [17].

Tendon does not deform more than 4% during everyday movements [7]. When tendon does not exceed that deformation the collagen pattern arrangement will resettle. Younger tendons usually fail under lower stress than mature ones. In rats' Achilles tendon, a crimp pattern is formed that varies between 0^o to 60^o and disappears when tension occurs [7]. The elastic energy storage is related to the stretching of that crimp pattern. Generally, it is debatable whether the transmission of force and energy dissipation occurs through proteoglycans linkages, or directly through the collagen fibrils [7, 23].

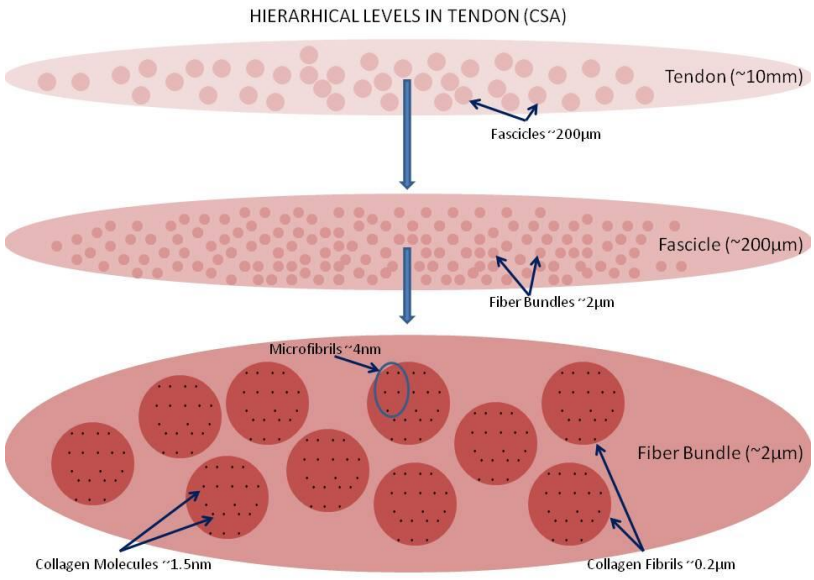

Figure 1. Cross-Sectional Area of all levels of hierarchy of tendon. At the top, tendon to fascicle, and fiber bundle to collagen fibrils. The figure shows the collagen microfibril arrangement.

1.3 Fibril Structure

Collagen fibrils in human tendons are made up of collagen type I, II, III, V and XI with type I being the most abundant. The final form of the collagen protein is that of a triple helix which is maintained by hydrogen, covalent and ionic bonds. The pair of charged interactions arrange in a quasi-hexagonal pattern. The molecules are crosslinked and thus mechanical loads are able to be transferred between them. Type I collagen is mostly found in skin, organs, tendon and bone. The complete formation of collagen fibrils occurs in the extracellular matrix [21].

The three-dimensional structure of collagen fibrils were investigated in the past with the aid of X-Ray diffuse scattering and quantitative computer tomography [1, 2, 3, 5, 6, 25, 36]. Each collagen molecule, along with its four neighbors, forms a rotating repeating unit, the microfibril [Fig. 2]. The formation of type I collagen molecule occurs with the synthesis of α-chains of about 1000 amino acids in length. It has regions at the N and C terminal ends, the propeptides that obstruct random aggregation. The C-propeptide controls which three α-chains come together to form the triple helix. Type I collagen consists of a sequence of two αI chains and one αII chain between them. Five groups of molecules comprise the collagen microfibril with a total diameter of 4nm approximately. Flexible tissues like blood vessels and dermis have helical microfibrils while stiff tissues like tendons have straight microfibrils [25]. Four out of five molecules form the gap region of 0.54D, while all five molecules form the overlap region of approximately 0.46D [Fig. 3]. The gap regions are represented by dark band in the X-Ray scans, as proposed by Hodge and Petruska, 1963 [36]. Units are labeled from one to five according to their

distance from the N-terminus and the collagen hole-gap zone [24, Fig. 2]. Segments of 3 to 5 molecules align adjacent to segments 1 and 2 [Fig. 2]. The diameter of the molecule is 1.5nm and has a length of about 300nm or 4.46D [24], (Fraser et al., 1983), while the center to center distance between molecules varies from 1.1nm to 1.7nm (Fratzl et al. 1993), [5]. D is equal to 67nm and 234 residues proposed initially from Hodge, and Petruska, 1963 [24, 36].

According to Orgel et al., in rat tail tendons the microfibrils are arranged on a discontinuous twisted way and they form a quasihexagonal pattern. With the use of an electro density map, the molecular resolution of collagen molecules was identified in situ within a unit cell of axial length D. Orgel claims that the microfibril can be described as a five 1D staggered molecules that are arranged on a right handed supertwist, appearing as a wavy lateral view pattern [1]. Thus, he proves that microfibrils are not separable units and for this reason it is hard to study their structure. Also, he confirms that each microfibril contains two to three intermicrofibrillar crosslinks and one intramicrofibrillar linkage. This explains the force and energy transmission through the lysine-hydroxyl-lysine crosslinks. Initial phase of a subunit self-assembly involves 5 to 17 molecules in lateral view and two to three molecules long. Thus, periodic subunits are formed in the lateral distribution of the fibril and each has a diameter of 4nm. In axial direction the collagen molecules are significantly regular. The packing of these units can be considered as continuous [1, 18, Fig. 2]. The present study is based on this specific packing arrangement.

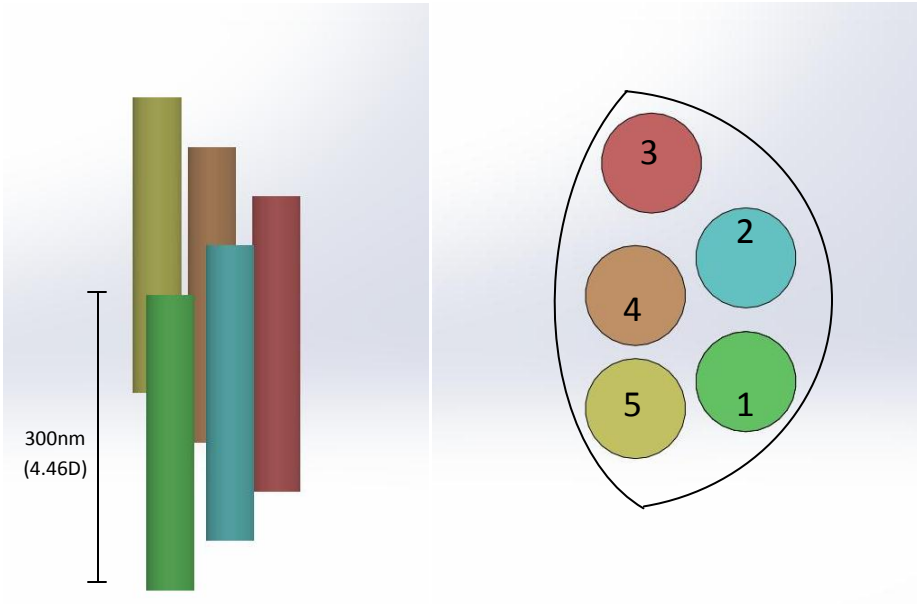

Figure 1. On the left molecular microfibril arrangement in three dimensions (size not on scale). Arrangement is based on Orgel et al., 2006. On the right, cross-section area of the microfibril. Each number represents specific level of each molecule in space.

The collagen tissue behaves as a viscoelastic material. The elastic part is attributed to the tension of the cross linked fibrils and depends on the fibril length as well as the number of crosslinks, while the viscous part involves the sliding of the molecules past each other. Fibril diameters are associated with the low strain modulus, while there is no correlation with the ultimate tensile strength or the high strain [18]. The increase in the diameter influences the mechanical properties and enhances resistance only for small deformations. Fibril diameters formed by in-vitro self assembly, also, depend on the pH [18]. The largest diameters appear for assembly at pH 5.0, while as the pH increased the diameter was observed to decrease [18]. The ultimate tensile strength was also higher for the fibers formed at 25^{o} C than those formed at higher temperatures [18].

Linear and lateral growth in collagen molecules occur by charged pair interactions that direct fibrillogenesis. Linear growth appears in D-staggered pairs between three molecules and occurs before the lateral growth begins. Increase in temperature leads to lateral growth [21]. X-ray diffuse scattering and computer simulations established the diversity of fibril packing arrangements between different mammal tissues. For example, in turkey leg tendons, the collagen packing in lateral plane is irregular compared to non-mineralized collagen rat tail tendons. In wet turkey leg tendon collagen appears more liquid-like than in dry tendon where there is a quasi-hexagonal pattern [5]. Inter-fibrillar fusion connections rarely appear at the ends of the fibrils. The length of the fibrils shows a frequency of 1 to 20000 D-periods of Y-shaped occurring branches with an angle of 4^{o} to 10^{o} in mouse tail tendon [10]. This implies that forces are transmitted directly between fibrils and can be observed through transmission electron microscopy. These branches could have a major impact on the tendon's mechanical properties and the interfibrillar connections could substantially increase the stiffness of the tissue [10].

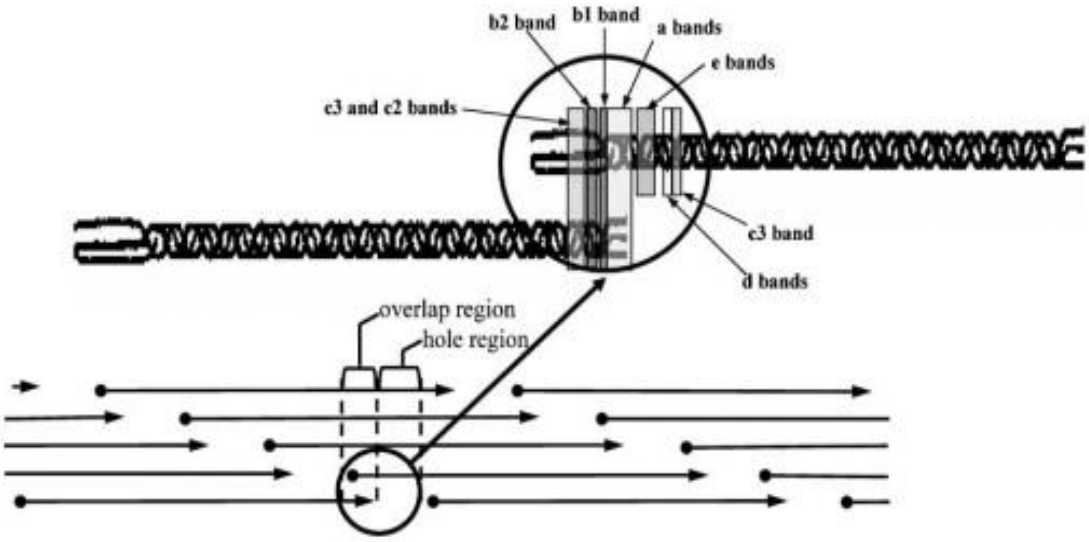

Figure 3. Collagen molecules. Arrangement of molecules in quarter-staggered pattern showing both overlap and gap regions, as well as the bands included in one D-period [Reproduced with permission from Silver, 37].

1.4 Crosslinks

The formation of covalent crosslinks improves the bonding of molecules in the fibril [15]. The enzyme lysyl oxidase initiates the crosslink generation. This enzyme catalyses the oxidative deamination of specific lysines on collagen to form allysines [12]. The amino group on the lysine reacts with the aldehyde on the telopeptide allysine to form a covalent bond [25]. Crosslinking takes place at both ends of the α1-chains but only at the N-telopeptide of the α2-chain and may be different between bone or tendon mineralization. The arrangement in the collagen aggregation ensures that two molecules are staggered by 4 D-periods and will have their telopeptide allysines next to lysine residues in the helical region of the other. Thus, the molecule has 11 possible sites of cross-linking, 3 N-

telopeptide, 3 N-helix, 3 C-helix and 2 C-telopeptide sites [Fig. 4, 25]. The mature cross-links are trivalent and may connect three α-chains on three different molecules creating a stronger fibril, or just two in the same molecule with one connected to another molecule's chain [Fig. 5]. According to the most recent packing model described by Orgel et al., in order to connect three molecules, two of them need to be in register [Fig. 5, 1]. The trivalent cross-links are formed between three molecules and not just three α-chains in two molecules [25, Fig. 4].

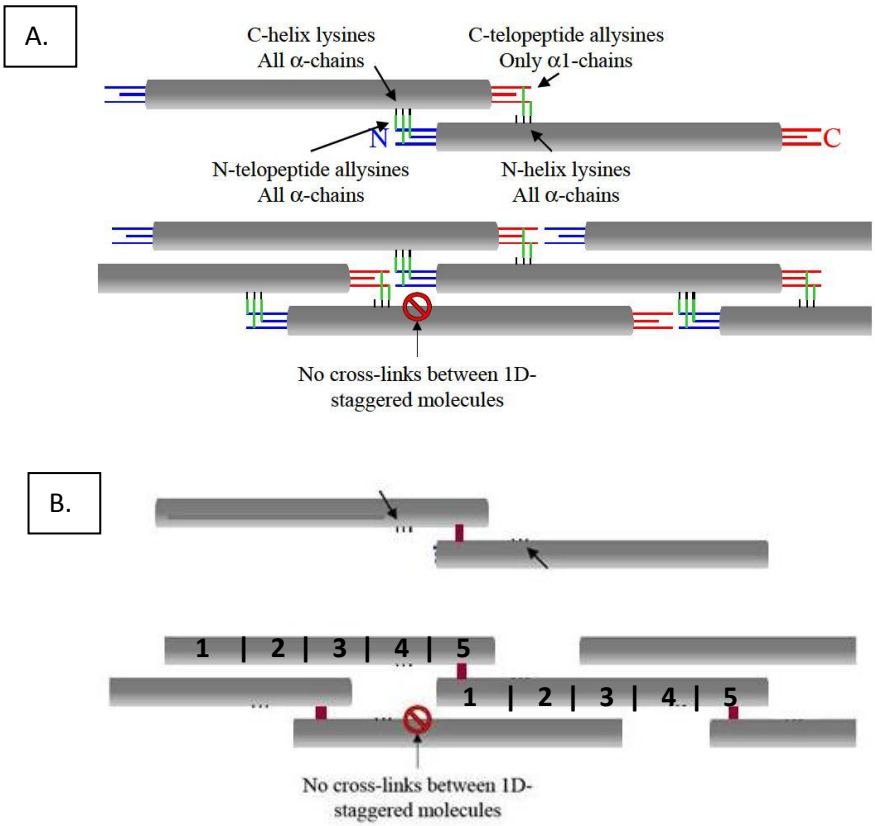

Figure 4. A., covalent crosslinking among 1 to 5 overlapping regions of 4D staggered molecules [Reproduced with permission from Svensson, 25]. B., crosslinking that is assumed and used in this study in order to eliminate the CPU time and complexity of geometry.

According to Bailey et al. (1980), the quasi-hexagonal packing problem of the collagen is unresolved without taking into account the crosslinks [12]. Thus, they suggest a model that follows the quarter stagger and overlap regions and impose the known locations of the intermolecular crosslinks. The molecules are staggered laterally producing row distance lines of approximately 3.78 nm. In this way they generate a pentafibril tetragonal unit cell by connecting the one to one and one to five molecule segments from right to left [Fig. 4&5]. This develops a two-dimensional lattice with distances equal to 2.6 nm and 3.9 nm approximately. In this study the molecules are connected in one to five segment levels for computational simplification and due to complexity of geometry. Crosslinking occurs at the end of the overlap region as well as the C-terminal of the non-helical region and the helical peptide α1CB5 between adjacent peptides. This way several layers can be interlinked repeatedly [12]. With increased crosslinking the mechanical properties show mainly an elastic behavior, while with less crosslinks the sliding of the molecules cause a viscous behavior. A decrease in swelling from crosslinks may increase the length of the fibril. Thus, higher crosslinking may eliminate the increase in D-period as tensile stress is applied [15]. In the study by Svensson et al., the failure of collagen fibrils suggests that divalent immature cross-links are not sufficient in blocking molecular slippage than trivalent mature cross-links, that support more efficiently the structure [25].

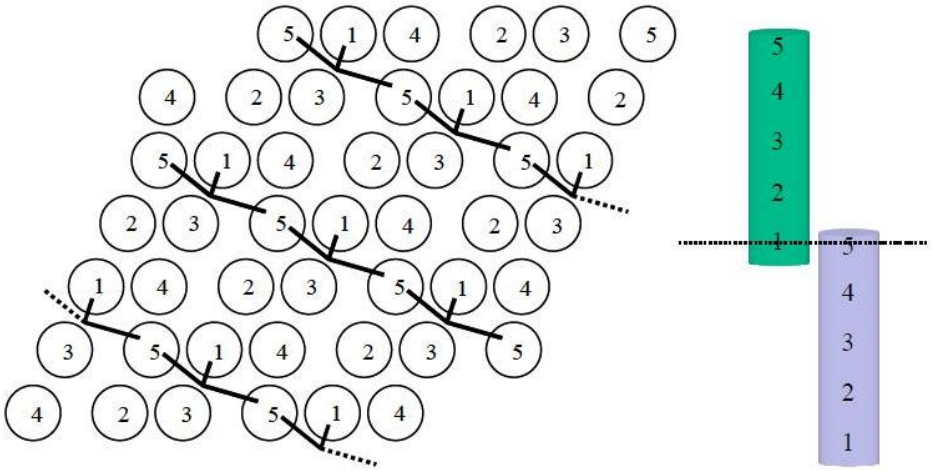

Figure 5. Crosslinking between three molecules showing five to five and five to one intermolecular connections [Reproduced with permission from Svensson, 25].

A model of collagen slippage with the crosslinks is suggested by Svensson et al. It is divided in three regions. In region I, non-covalent interactions at the molecular interfaces are able to withstand the applied force without slipping and the modulus and stress rises as the molecules are stretched. In region II, the non-covalent interactions are no longer strong enough and the molecules start slipping relative to each other thus producing a plateau in the mechanical response. In region III, the slippage is stopped by covalent cross-links and the molecular backbone is stretched causing the modulus and stress to increase again until final failure [25, Fig. 6]. Finally, formation of crosslinks within the fibril leads to potential increased stretching and decreased slippage of the molecules. Decorin and Proteoglycans enhance the linking and arrangement of the molecules [17].

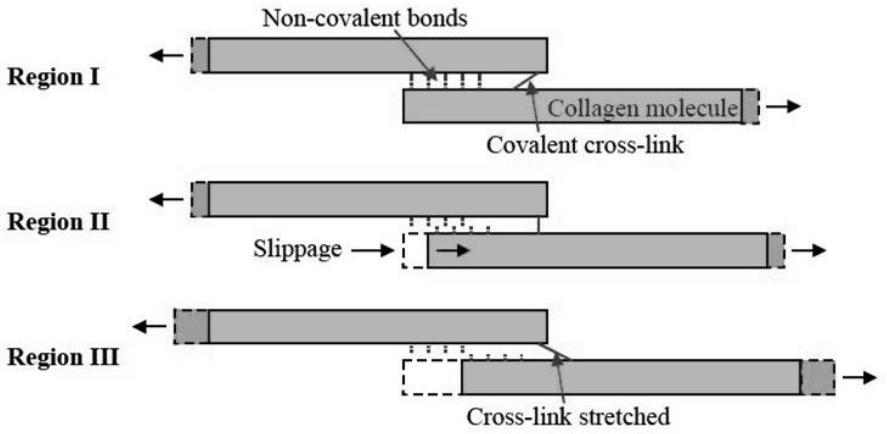

Figure 6. Proposed elongation structure of three phases by Svensson et al., [Reproduced with permission from Svensson, 25].

1.5 Mineralization

Collagen molecules facilitate the mineral formation and act as a template. It is known that crystal growth occurs in the gap and overlap zones. Mineral is initially located in the gap zone and as mineralization continues more crystals are formed within the overlap region pushing the molecules, and thus increasing the stored elastic energy [5]. Parts of the regions of the collagen molecule are different in flexibility. In general, it is considered that the elastic modulus of collagen type I does not change with mineralization. However, the terminals of the molecule and the crosslinks tend to be more rigid. Thus, the parts of the molecule with the Gly-Pro-Hyp sequence are more rigid. Moreover, rigid regions of the collagen are found to be at the end of the molecule. Parts of the molecule that do not

include the amino acids proline end hydroxyproline, such as the hole region that contains the d and e bands are more flexible. Mineralization is also responsible for the change of mechanical properties in microfibril level as well as some geometric changes. The lateral intermolecular distance is found to be 1.6 nm for wet and 1.1 nm for dry state [5]. Bragg spacing also decreases almost to 1.24nm when the tendon is wet and mineralized and thus it is reduced to the same value of dry tissue [5]. The modulus is maximum when the pH is close to 9.0 and suggests that mineralization increases the stiffness of the fibrils [19]. In the study of Silver et al., 2000, they showed that mineralization did not change significantly the elastic properties of the tendon [16].

The crystals of the mineral apatite resemble small platelets and form initially in the hole zone channels, while they rearrange in their own directions. Furthermore, they can originate in the overlapping regions, too [Fig. 7]. The formation of numerous hydroxyapatite (HA) platelets arises from the mineral-collagen interactions. The paradox is that the gap regions are about 1.5nm in diameter and 36nm in length, while the hydroxyapatite crystals are 50nm long, 28nm wide, and around 2nm thick. Therefore, there is a special rearrangement of type I collagen molecules that enhances the growth of crystals in a coplanar way with the help of the flexibility of the triple helix as well as the crosslinking arrangement [33].

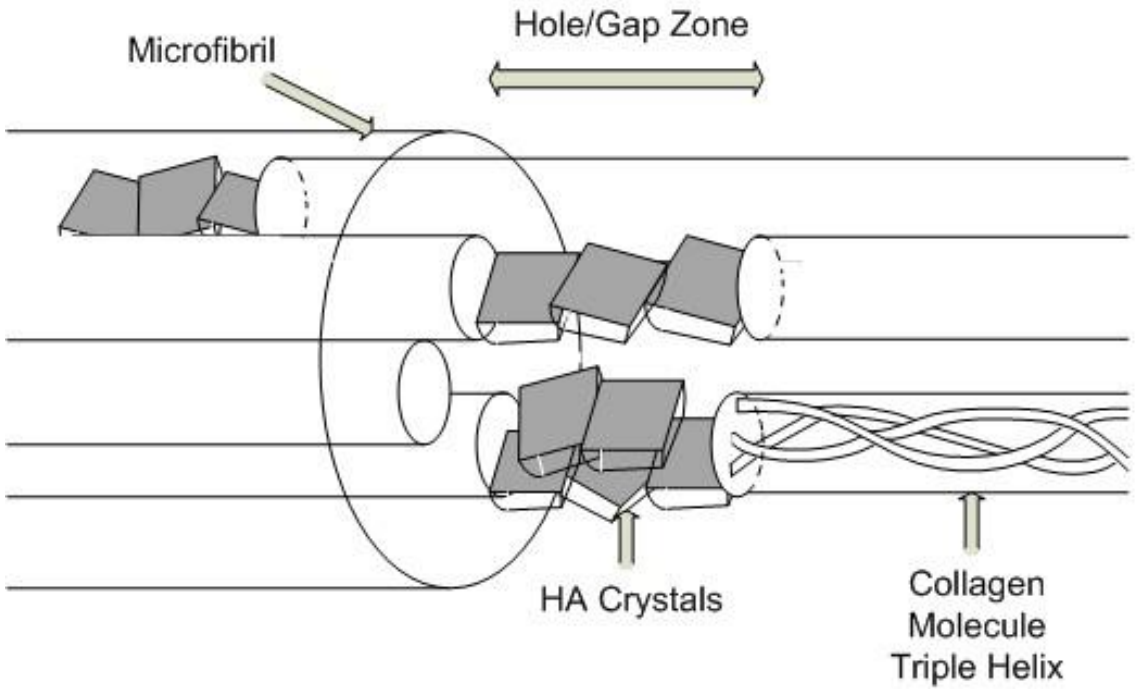

Figure 7. The hierarchical structure of assembled hydroxyapatite between collagen fibrils.

The organization of collagen molecules with the hydroxyapatite crystals in the first level of hierarchy occurs initially in the hole zones. In the second microfibrial level of hierarchy, the mineral crystals grow in the continuous longitudinal axis of the fibrils, as well as on their surface [33]. In this study we set the mineral to connect the microfibrils only in the gap zone and not among their long surfaces. Finally, in order to form the mineralized collagen fibers a plethora of mineralized collagen fibrils have to align in parallel [Fig. 7].

CHAPTER 2

MECHANICS

2. MECHANICS

Many experimental tests in the past have estimated tendon's mechanical properties and most of them have focused on the elastic response. Moreover, in many studies the approach that was used involved the load applied and averaged to several fibrils [3]. It is widely observed in previous studies that tendon's behavior at low strain shows a curve in the stress-strain graph with a slowly increasing slope before reaching the linear part. This is called toe-region and is related to straightening out the fibrils, which in the relaxed position lie in a wavy pattern.

Sasaki and Odajima, used X-ray diffraction in bovine Achilles tendon collagen [2, 3]. In the experiment, the force-strain curve in the D period showed that the gap period was Hookean type, while the overall results after macroscopic loading for the tendon was non-Hookean. Force strain curves were obtained for macromolecule, fibril and tissue deformation. In this work, the authors report that the steep region of tendon's curve is linear and similar to the collagen fibril's slope which gives a Young Modulus of $E=4.3x10^9$ dyn/ cm^2 or 0.43 GPa. Their Young modulus of collagen molecule is claimed to be much larger than that of the fibril level, E = 2.9 GPa [2, 3]. Thus, mechanical properties and overall loading contribution should be understood in each hierarchical level of the tendon's tissue. Specifically, molecular deformation is associated with the elongation that results in molecular rearrangement and change of D-period structure, as well as gap increase and slippage of neighboring molecules laterally [2, 3]. Furthermore, there is an approximately linear association of the ultimate tensile strength total, elastic, viscous slopes with the volume fraction.

According to Silver et al., the elastic stress can be defined as the stress in equilibrium and the viscous can be estimated from the difference of the total-elastic stress [15]. In the study of Silver et al., (2000), the authors showed occasions in which stresses varied from 0 to 80MPa with a relative strain increase from 0 to 0.12. The total stress-strain slope for mineralized tendon was determined to be 443MPa, while the elastic slope increased from 0.7 to 387MPa. The length of the fibrils ranged from 416 to 616μm. In the same study the elastic spring constant for the collagen molecule was estimated to be between 5 and 7.5GPa [16]. In the current study the initial elastic molecule modulus used for the first four models is obtained from Sasaki and Odajima, 2.9GPa and for the fifth model from Silver et al., 7GPa [16].

Tensile strength depends on the diameter of the fibers. Collagen can be found in dermal repair tissue in higher proportion relatively to the tensile strength that is applied. Low strength is responsible for forming smaller diameter fibers, while applying an instant force contributes to bigger diameter fibers and increased toughness. It is known that the fibers network aligns according to the stress directions. Generally, it is observed that the diameter of the fibrils and fibers is less in the scar tissue than that of normal tissue. This is proved in a study that reports that after six months of wound healing the collagen fibers approached a diameter of 12.6μm which was not the same as the fibers in the deep zone of normal dermis, 15.7μm. The packing density from the beginning of the healing phase remained the same as the collagen network developed [14].

2.1 Elasticity

The most frequent structural protein in tendon skin and bone is collagen type I, which is responsible for these tissues' mechanical behavior. In many experiments done with X-ray scattering measurements of rat tail collagen fibrils and tendon, the stress-strain curve showed that strain deformation was larger in tendon's collagen fibrils, which implied that deformation occurred inside the proteoglycan matrix between the fibrils. The toe region in those curves belonged to the initial values of stress that did not contribute to elongation [2, 3].

Stress-strain curve in tendon exhibits three regions. The first appears at small strains the toe region. The second is the heel region where a significant increase of stiffness appears, since linked molecules straighten. The third is the linear region where collagen molecules slide past each other [6]. It is claimed that there is wide range of axial deformation. D periods may increase from 0.2nm to 2nm before fracture [17]. The proteoglycan matrix becomes stiffer after increased strain rate. Moreover, crosslinks are critical in identifying the fibrils' stiffness. The Young's Modulus, also, depends on the tendon's type. The Young's Modulus of the rat tail tendon molecule was reported to be 7.7GPa. The authors claim that the elastic constant of the molecule is most likely higher. The tendon's mechanical properties change with age because fibril length and diameter increases [17].

According to Silver et al., the elastic behavior is attributed to the stretching of the cross-linked collagen molecules, while the viscous behavior is due to sliding of the molecules and fibrils that pass each other. It is reported that at the region of high strain of skin tissue stress-strain curve, the increase in the pH leads to higher elastic modulus, while decrease reduced the modulus. This occurs because the total charged residues increased with higher pH, and thus the elastic modulus is directly related to the number of total surface charges [20]. The sequence of Gly-Pro-Hyp is responsible for the rigid parts of the molecule. Intermolecular electrostatic interactions between charged pairs of neighboring collagen molecules lead to stiffening. Crosslinks contribute to the reduction of many charged residues, which leads to an increased flexibility. In the same study from Seehra et al., the elastic spring constant for dermis was reported to be 3.4GPa [20].

2.2 Viscoelastic Properties

Viscoelasticity occurs when the stress-strain behavior depends on the rate in which the material is loaded. Viscoelasticity is caused by rearrangement of molecules to reduce the load by slippage or unwinding. Rapid loading will allow less time for rearrangement than slow loading resulting in greater forces. The Young's modulus in tendons appears to increase with strain rate [3]. This proves the viscoelastic nature of collagen [3]. Viscosity is, also, related to the axial ratio of the macromolecule [16]. Thus, there is a viscoelastic component in the mechanical behavior of collagen molecule since the strain is observed within the molecule.

The intra molecular stability is provided by hydrogen bonds that are bridged by water molecules. Breaking and reforming of these bonds occurs when the tendon is hydrated. This contributes to energy dissipation and results in the viscoelastic behavior of the collagen because of the stretching and molecular slippage [3]. When stress is first applied there is unwinding and straightening of the collagen molecules. Then they slide past each other while the water molecules may rotate and translate inside the fibril. In the study of Shen et al., an elastic modulus of only 123 MPa is reported, from creep and relaxation tests on collagen fibrils of sea cucumber dermis, using a Maxwell-Weichert model [9]. After the first test of the specimen the elastic modulus gradually decreased. It is considered that with only two times of loading-unloading the fibrils is enough to show the mechanical response. The initial stretching strain of each specimen was 21% and the engineering strain showed a rapid increase at the beginning of the test [9].

Studies that use the atomic force microscopy method may fail in a non-axial loading of the fibril with the probe tip. Moreover, it is claimed that one of the most widely used model to describe more appropriately the viscoelastic behavior of tendon, is Fung's Quasilinear Viscoelastic model [9]. In the study of Shen et al., the stress-time and strain-time curves of the curve fitting data showed the viscoelastic behavior of the collagen fibrils. The viscosity was found to be 0.09-1.63 GPa*sec [9]. According to Silver et al., the viscoelastic mechanical properties depend mainly on the length of the fibril rather than the diameter [17]. The Elastic modulus of the fibrils is characterized by the covalent crosslinks while the viscosity is provided by friction of the molecules and hydrogen bonds interactions [6]. Finally, an increase in the pH results on increased modulus [20].

2.3 Energy Transmission

Collagen tissues are responsible for force transmission. However, force transmission is still not fully understood in smaller scales. Experiments focusing on shearing between molecules and their sliding mechanisms in dry and solvated conditions, show that in dry condition the stretching of the molecules is responsible for the elongation of the fibril, which leads to higher stiffness [4]. On the other hand, in hydrated state the water provides the shear between the molecules [4]. The viscous component depends on possible water mediated sliding, while the triple helix molecule stretching is associated with the elastic behavior. There is insuficient knowledge on how water contributes to load transfer within the fibril. However, it known that there is less formation of H-bonds in hydrated state and water molecules act as a lubricated medium to transfer load by forming water bridges between collagen molecules [4].

Tendons are often viewed as fiber reinforced composites with collagen fibrils as the fiber reinforcement and the proteoglycan gel acting as the interfibrillar matrix. One of the primary factors influencing force transmission is the length of the fibers, if they are discontinuous load has to be transmitted between them, and the structures responsible for this force transmission can become a weak link. Several studies have found implications that fibrils in tendons are indeed discontinuous. This hypothesis of discontinuity of the fibrils gives rise to questions of existence of a mechanical linkage responsible to transmit forces between discrete fibrils. Even though force transmission is possible through the friction of the fibrils, molecular linkers could also be an approach. One of the major

fibril-connector is the proteoglycan decorin, which has a core protein in a horseshoe shape that binds to collagen fibrils and a single glycosaminoglycan (GAG) chain. However, Svensson et al.'s findings in combination with other studies show that GAGs are not required to transmit force between fibrils in the sub-failure regimes [25].

2.4 Steered Molecular Dynamics

In the literature, apart from the widely used experimental methods of X-Ray diffraction and atomic force microscopy, the recent computational method of Steered Molecular Dynamics (SMD) is rapidly developing. Many efforts of estimations of the mechanical properties and behavior of collagen are made using the molecular dynamics software. Gautieri et al. simulated, with the help of SMD 7 molecules in hexagonal packing, in which he pulled the one in the center. The shearing tests in dry state showed that when the molecules were tight with 1.1nm intermolecular distance, the sliding occurred for more than 15nN force. Thus the elongation of the fibril was attributed mainly to molecular stretching [4]. Lorenzo and Gaffarena, 2005, performed steered molecular dynamics simulations in collagen Pro-Hyp-Gly peptide to measure the elastic properties of collagen molecules in the longitudinal axis. They report a linear elastic response for the first 4% deformation and an elastic modulus at 4.8 GPa. The elastic modulus was calculated using a simple model of two springs in series. The three chains in the molecule were held together mainly by 94% of the total amount of hydrogen bonds [8]. In the study by Zhang et al., 2007, with the use of steered molecular dynamics, they confirmed

that the water is a weak means of transmitting axial tensile load [11]. Instead, they claim that it functions as “glue” in axial sliding and bending. Energy of continuous breakage of the hydrogen bonds increases the water resistance. At molecular level, they also consider water molecules to be responsible for stabilizing the structure. It is observed that the force-displacement curve has a toe region shape under axial stretching, while the water provides a slight lubricant effect. The Young modulus was estimated to be 6.5 GPa with no intermolecular interactions. They also reported that the force under bending was significant higher when water was included in the experiment. The water has a glue effect when there is bending or sliding of the molecules [11].

Gautieri et al., 2012, used steered molecular dynamics and performed creep tests showing strain-time response under various loading. The results report a viscoelastic behavior and a Young modulus in solvated condition from 6 to 16 GPa for strains up to 20% and 10 to 19 GPa for the dry condition. The viscosity was estimated to be 3.84 Pa*sec for solvent molecules and 2.64 Pa*sec for the dry environment. This viscosity is considered to be several times lower than the one of larger scale fibrils. In order to fit the data the authors use a Kelvin-Voigt model to identify the Young’s modulus and the viscosity. They performed the experiment for both wet and dry single collagen peptides on which they applied an instantaneous constant force varying from 300 pN to 3000 pN. The elastic spring constant of the Kelvin-Voigt model corresponds to the molecule deformation. The damping viscous effect is assumed to be related to breaking and forming of the Hydrogen bonds between the collagen chains. The average Elastic modulus of the collagen fibril is reported to be equal to 0.90 GPa. This is six times less than the molecular level where the

Young's modulus is estimated to be 5.40 GPa. Their model did not demonstrate the time dependence of the fibril mechanical response, thus they conclude that the viscous effect depends on other mechanisms such as sliding of the neighboring molecules. Finally, they reported that the relaxation mechanisms and the time scales they found may not be visible in such small scale simulations [13].

Table 1. Elastic Modulus reported in literature for the small scale levels.

	Study	**Type/ Hierarchy**	**Elastic Modulus**	**Year**
Experimental, Emperical	Sasaki and Odajima	Macromolecule Collagen fibril	2.89GPa 0.43GPa	1996
	Silver et al.	Macromolecule	5 to 7.7GPa	2000
	Seehra et al.	Dermis fibrils	3.4GPa	2006
	Shen et al.	Collagen fibril (Sea cucumber dermis)	123MPa	2011
Steered Molecular Dynamics, SMD	Lorenzo and Caffarena	Microfibril	4.8GPa	2005
	Zhang et al.	Microfibril	6.5GPa	2007
	Gautieri et al.	Microfibril Macromolecule	0.96GPa 5.4GPa	2012
Finite Element Analysis, FEA	Hambli and Barkaoui	Microfibril	1.9GPa (dry) 0.26GPa (wet)	2012

CHAPTER 3

FINITE ELEMENT ANALYSIS

3. FINITE ELEMENT ANALYSIS

Prediction of mechanical properties in nanoscale is of outmost importance and needs a cautious approach. All experimental measurements of the mechanical properties of microfibrils are a tedious task in such a low scale. As a result, modeling and simulation methods are crucial in determining their properties and their mechanical behavior [29]. In the preprocessing stage, the model is divided in discrete small parts called elements, and each element in three or more connective nodes depending on the dimensions and geometry of each element. The software solves a system of linear or nonlinear algebraic equations for the displacements of each node. The equations are described from $K_{ij}u_j=F_i$, where u_j are the displacements of each node and F_i their respective forces applied on them. K is the analysis global stiffness matrix, that is analogous to AE/L, thus depends on the geometry and modulus of each element and feature [27].

In general, it is possible to classify simulation methods into atomistic and continuum techniques [29]. Atomistic modeling techniques are solved with the use of Schrodinger equation or Newton's second law. The latter is called molecular dynamics as previously referred in chapter two. With these methods the mechanical properties are estimated from a force or energy approach. Furthermore, this atomistic technique can be useful to spot deformations in a scale of an order 10^{-9} and under short times. This approach has increased computational requirements and thus its use is restricted to a low number of atoms [29].

On the other hand, continuum modeling employs well developed theories of elasticity by simulating the geometry as plates, beams, and rods. Substituting a molecular structure with a continuum geometry is difficult and one of the most crucial parts of the process. Thus, these continuum methods can be applied to nanoscale given a successful association of the molecular behavior with the solid mechanics. This is defined as a nanoscale continuum technique and is a preferred method to model nanostructure materials [29].

The present work evaluates different numerical models, which simulate the mechanical behavior of the collagen microfibrils. Regarding the mechanical and geometric properties of the network, the proposed approach adopts numerical values from the literature after careful consideration. The geometry is specified in space according to the packing model by Orgel et al., 2006. More specifically it represents the rat tail tendon or mineralized turkey pattern. All models consist of two distinct volumes, corresponding to the portions of the crosslinks and the collagen molecule backbone. The models' differences relate to the geometry of the different features, mineralization and hydration, as well as on the mechanical behavior of the materials of each portion. The exerted loads model the standard loads used in experiments and were obtained from previous studies in literature.

The study is based on the use of the finite element method with the aid of the student version software ANSYS Workbench, Inc. Release 14.0, November 2011. The assumptions that were made regarding the mechanical and geometrical behavior of the material of the crosslinks and the collagen are based on literature and previous studies.

The adopted geometry is a simpler version of reality. Nevertheless, there are no clear outcomes, even today, regarding the exact form of the boundary condition for each level and molecular region. Thus, this challenge is still actively researched.

3.1 Background

Detailed CAD models and finite element models (FEMs) of collagen network in three dimensions are still lacking. FEM provided less computational time than molecular dynamics simulations, up to 25 minutes including more geometrical features than SMD. Bending, torsion and shearing simulations would be less tedious with the use of FEM since there are limitations with experimental devices. In this study our representation of the microfibril consists of five collagen molecules with intermolecular crosslinks and hydroxyapatite, while there is a cross sectional repetition of the microfibril pattern. The focus lies on the creation of a 3D realistic model in the microfibril level and its validation with experimental data obtained from literature. Finite element analysis is used to identify the soft tissue's structural response in the elastic small strain regime for small deformations, $\varepsilon < 5\%$.

In the study of Hambli and Barkaoui [22], they tested a single microfibril in the elastic regime with cross-links that were considered to be spring elements connecting two random molecule terminals and their interfaces. Our study follows Orgel's packing, while specific crosslinking and staggering based on Bailey et al., 1980, is implemented [12].

The sliding effects between the mineral and the collagen were neglected for the simplification of boundary conditions and reduction of surface elements. Also, water is of small percentage in the mineral phase and thus it is neglected. Hambli and Barkaoui's model included 22,000 quadratic tetrahedral elements for higher accuracy, while ours is up to 16,188 due to license limitations. The model was constrained to avoid buckling in compression test. The boundary conditions that were applied have the one side fixed and the other tensile loaded. The length of their model was 340nm and the diameter 4nm, while in this study the overall model is 300nm in length and approximately 0.024μm wide [22].

The mechanical properties used for the collagen molecule are E=2.8GPa with a Poisson's ratio ν=0.30 obtained from Sasaki and Odajima, 1996. In Hambli and Barkaoui's study for assigning the mineral material they use linear isotropic materials with E=114MPa and ν=0.30, while we are using the Hydroxyapatite Elastic modulus of 20GMa and 0.25 Poisson ratio that is reported for bone. They conclude that the increase in mineralization also increases the stiffness of the bone. Collagen network enhances the tensile strength, while the mineral provides rigidity in compression. They report a Young's modulus of 1.9GPa for dry state and 0.26GPa for hydrated state, thus their elastic modulus is highly influenced by the state. Furthermore, they mention that in compression the microfibril is 3 to 7 times stiffer than in tension. The stress-strain curves in tension and compression were found to be linear, with higher stiffness for the compression test. Thus, the mineral in the gap region enhances the stiffness under compression [22].

3.2 Methods

The fibril model is undergoing a mechanical test that involves placing a material under load and determining how much it deforms in response to that load. The relationship between force and deformation define the mechanical properties of that object. The load may be applied along any direction, but in the present work we use only tensile loads across the longitudinal axis. The molecules are represented by long cylindrical structures with a ratio of diameter/length equal to 1.5/300= 200.

A generally accepted approach to comprehend force transmission in tendon is to compare the properties observed at different hierarchical levels. Knowledge of the mechanical properties of the individual collagen fibrils and of tendons makes it possible to finally realize the system of force transmission. In the present study we performed tensile tests in the elastic region with 5% strain, thus, producing linear stress-strain curves.

To determine material properties the force and deformation has to be normalized to the size of the tested object. The normalized force is the stress (σ) defined as force divided by area (A).

$$\sigma = \frac{F}{A} \quad ,$$

For tensile testing of a cylindrical object like a tendon or fibril, the area in question is the cross-sectional area of the force applied. Furthermore, the normalized deformation is the strain (ε) defined as deformation (Δl) divided by the undeformed length (l_0) of the

specimen. In our case, of the fibril model under tension, this length is simply the length of our total model equal to l_0=300nm. The SI unit of stress is N/m^2 or Pascal (Pa) and the strain is unitless but usually it is reported as a percentage.

In the stress-strain curve there is a linear region, which has a slope that defines the modulus (E) the total material stiffness. A small slope corresponds to an extensible material and a steep to a rigid one. In the linear region the material components can deform remaining intact and appropriately organized, making deformation in this region reversible. In the stress-strain graph the area under the curve has units of energy per volume and corresponds to the mechanical energy dissipated into the material. To avoid damaging the material, mechanical testing is commonly performed in the elastic range. Such tests are often cyclic with the material being repetitively loaded-unloaded.

3.2.1. Geometry and Packing

The geometry of all the models is based on Orgel's microfibril structure, 2006. The microfibril consists of five molecules parallel in space each 1D distant on z-plane from each other and 0.6D separate from the next continuous microfibril, along the longitudinal axis. This pattern was repeated for 6 more microfibrils along x-axis and two more along the y-axis, thus having a total of 12 microfibrils in cross-section, or 120 solid bodies of collagen molecules [Fig. 8 & 9]. With this patent we eventually get a total length of 300 nm that is divided in five overlapping regions as shown in Figure 8.

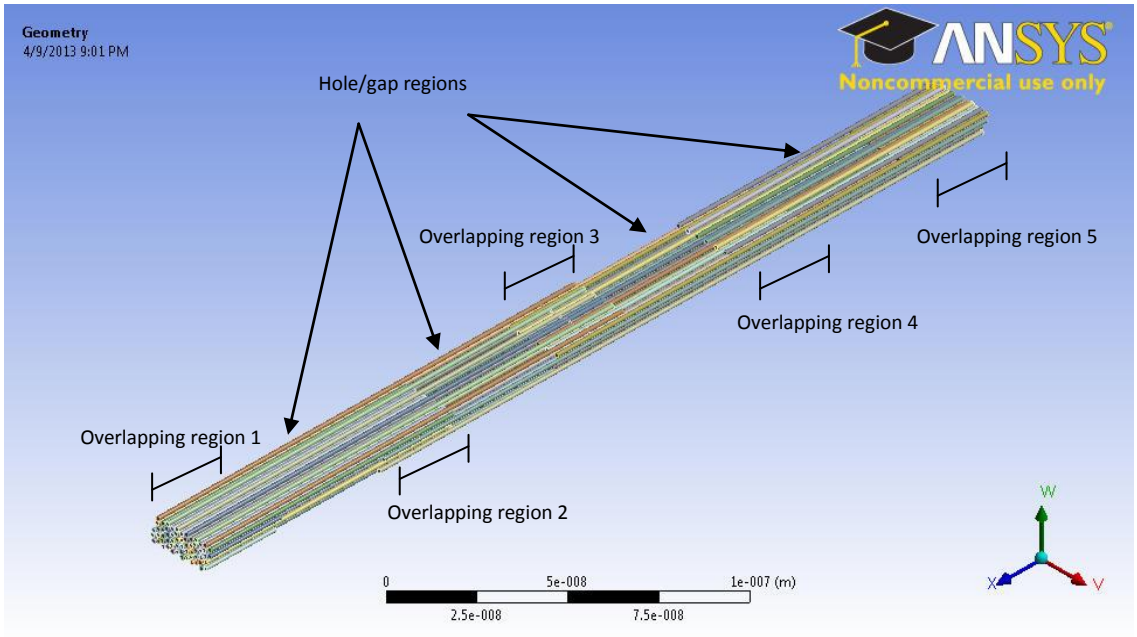

Figure 8. The final model consisting of the five overlapping regions and four gap zones.

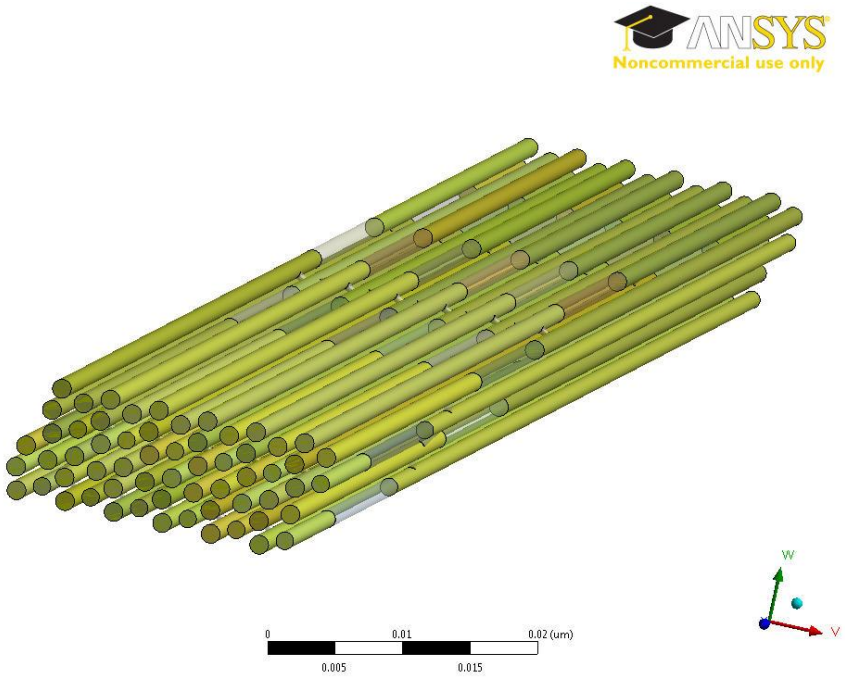

Figure 9. Final model showing all collagen molecule bodies with the gap regions, no mineral.

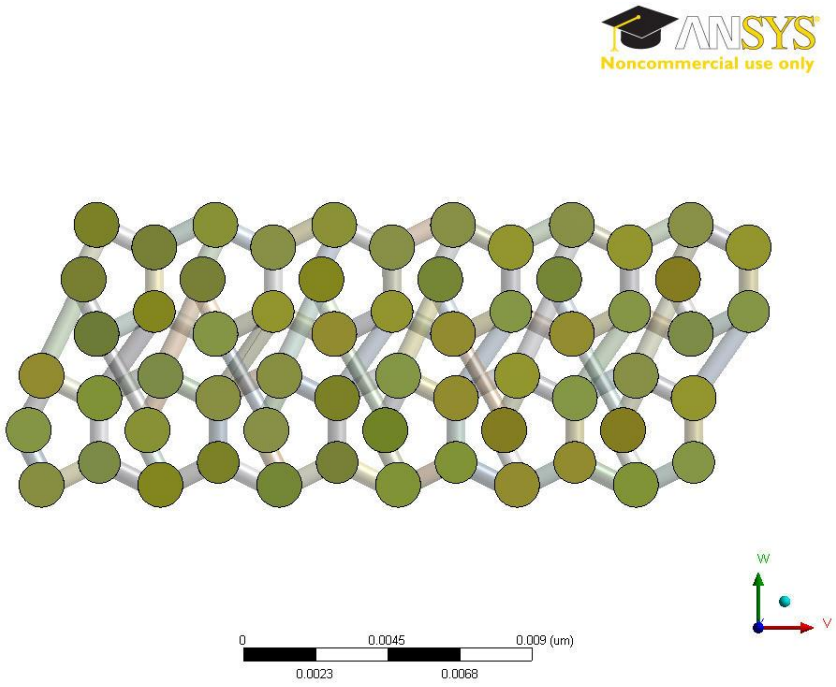

Figure 10. Cross-sectional view of final model showing the projected molecular packing and crosslinking of all overlapping regions in depth.

For the models that the mineral is included, additional cylinders are placed that connect the microfibrils along the z-axis and fill the hole-gap regions. Also, for the dry dehydrated models, the molecule diameters were decreased to 1.1nm as shown in figure 11. From the cross-sectional figures all of the crosslinks are apparent and demonstrated for all five regions in depth [Fig. 10 & 11]. Crosslinks are shown separately for each region in the appendix.

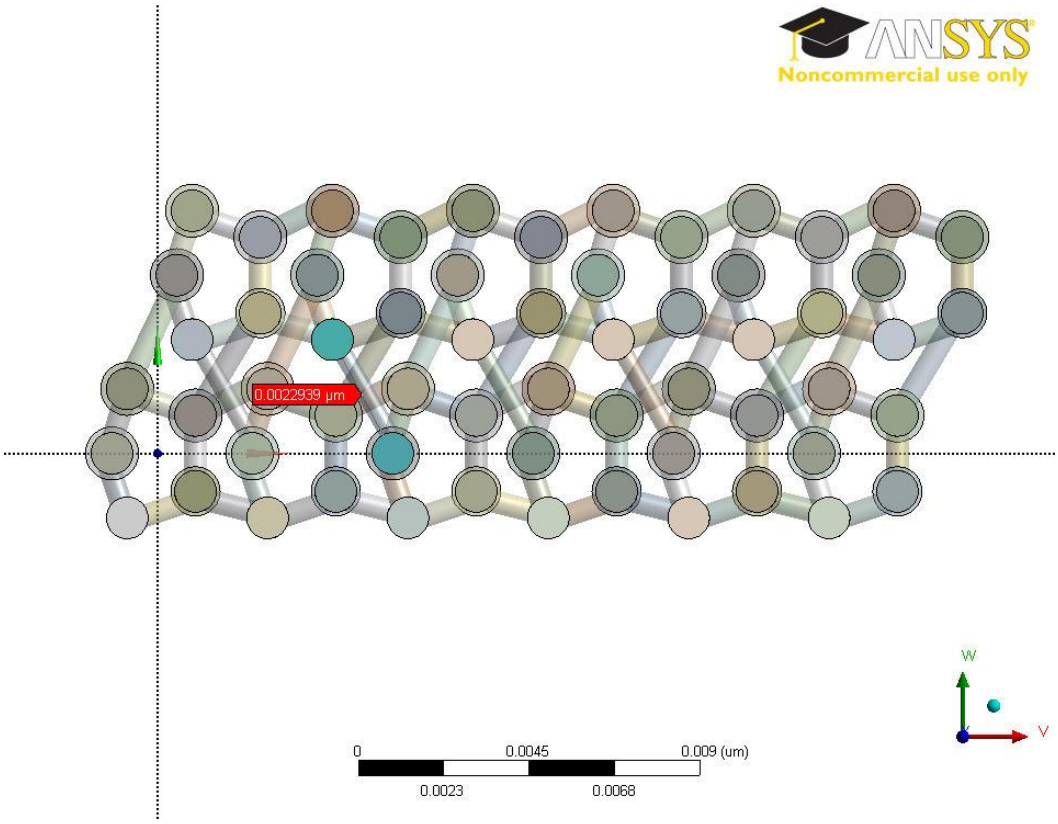

Figure 2. Cross-sectional view of dehydrated model with mineral, projected view.

3.2.2 Cross-linking

Apart from the mechanisms that govern force transmission through tendon, we also have an interest in understanding the mechanisms governing force transmission through individual collagen fibrils. A fundamental aspect of this are the cross-links involved in interconnecting collagen molecules throughout the length of a fibril. The importance of cross-links for connecting otherwise disconnected molecules in a fibril is conceptually obvious and has been shown in terms of increased collagen thermal stability, decreased solubility and resistance to proteolysis as well as increased mechanical properties at the macroscopic level.

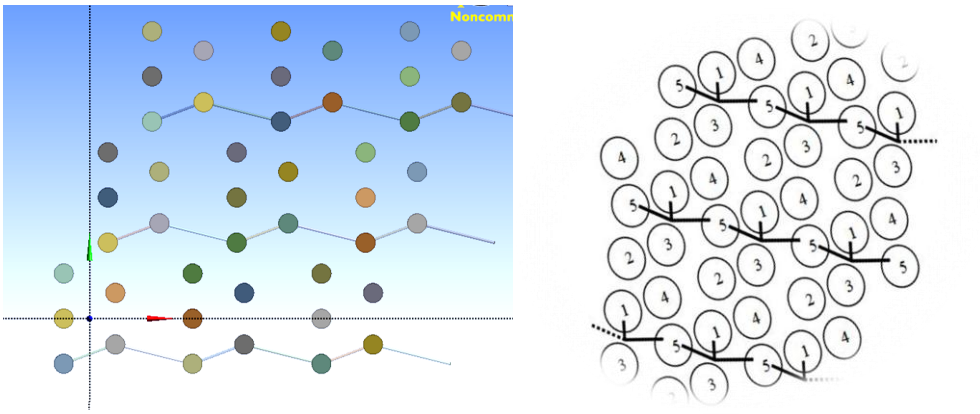

Figure 3. Left, current models' crosslinking of first overlapping region of 5 to 1 staggered molecules, according to Bailey et al. [12], and Svensson et al. shown on the right. [Reproduced with permission from Svensson, 25].

Our crosslinks are placed on locations that bond 5 to 1 regions of the molecules according to Bailey et al., 1980 [12], and extend from 0.3nm to 2.2nm depending on the overlapping region that they exist and the lateral distance of the two staggered molecules that they have to connect to [Fig. 12].

3.2.3 Mesh

In general it is proven that quadrilateral elements converge faster than triangular elements [28], thus in three dimensions the convergence speed of hexahedra is faster than prisms or tetrahedral. In 3D the total degrees of freedom equal three times the number of nodes. Hexahedra elements are more preferable than other shapes. This happens because with the same problem size these elements give more accurate results and they need less iterations in nonlinear simulations. In 3D cylindrical shapes meshing is more challenging. Automesh in ANSYS-Workbench chose to mesh all the molecules and crosslinks with all-tetrahedral. The lower order tetrahedral elements are considered to converge very poorly. Choosing higher order elements results in a rapid increase of nodes that made the model more complicated and unable to solve since there was a limitation of size of nodes that could be used due to the license type and version of ANSys software. Computational time is a major issue that depends also on meshing. For the simulation part the computational time is divided in three parts. The first one is the time that is required to establish and involves the numerical integrations element to element. The second is the

time required to solve the equation and is determined by the number of degrees of freedom, which is calculated from the number of nodes and the dimensionality. Thirdly, we have the actual post processing solution [26, 28]. Tables 2 to 4 show the exact numbers of elements and nodes created for each model's feature in detail, as well as the overall computational time.

Table 2. Meshing Details for Hydrated No Mineral Model.

MODEL 1&2	Collagen Molecules	Mineral in Gap Region	Cross-links	Total	CPU Time
Elements	2,712	N/A	4,785	7,497	20 min.
Nodes	33,408	N/A	29,304	62,712	
Bodies	108	N/A	97	205	

Table 3. Meshing Details for Hydrated with Mineral Model.

MODEL 3	Collagen Molecules	Mineral in Gap Region	Cross-links	Total	CPU Time
Elements	2,712	7,410	4,785	14,907	25 min.
Nodes	33,408	41,220	29,304	103,932	
Bodies	108	48	97	205	

Table 4. Meshing Details for Dehydrated with Mineral Model.

MODEL 4&5	Collagen Molecules	Mineral in Gap Region	Cross-links	Total	CPU Time
Elements	2,712	7,392	6,084	16,188	20 min.
Nodes	33,408	40,992	36,086	110,486	
Bodies	108	48	97	205	

ANSys automesh initially divided the structure in more than 100,000 elements. To overcome this problem we used the multi-zone meshing feature which decreased the elements to the numbers mentioned in the above tables by creating sweepable bodies.

This results in reducing significantly the number of the elements since our main bodies are sweepable cylinders [Fig. 13 & 14].

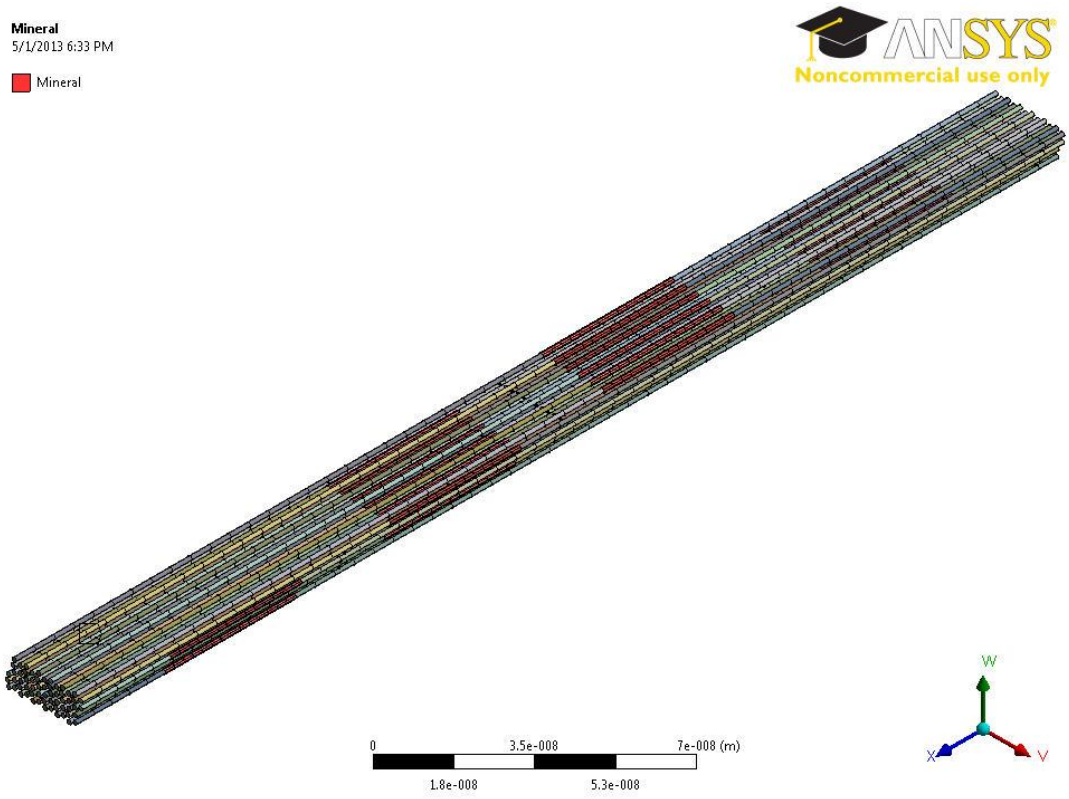

Figure 4. Meshed model showing mineral regions in red.

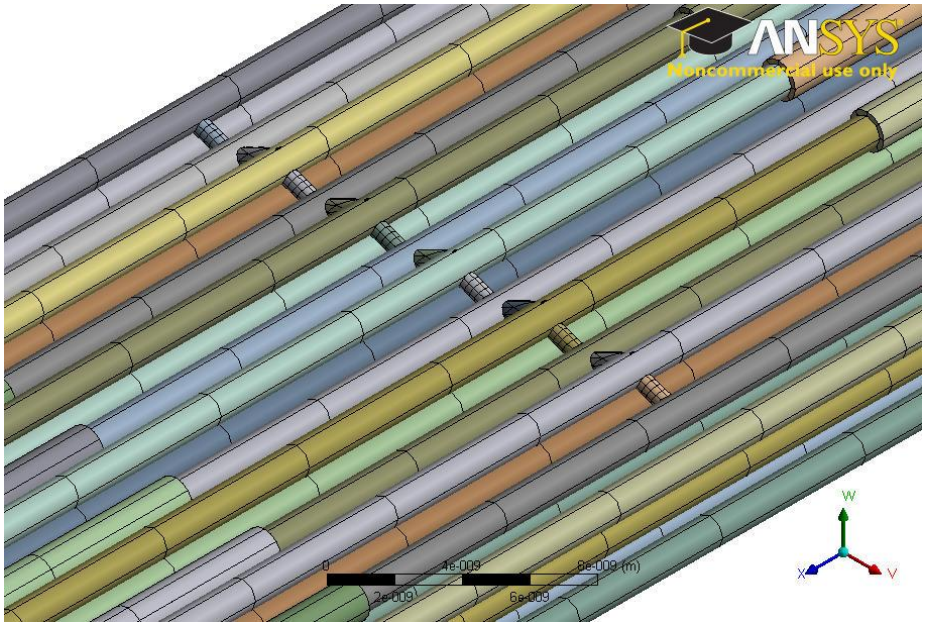

Figure 5. Detailed mesh of crosslinks, mineral and molecules.

3.3 Materials

The mechanical and material properties of collagen are still debatable because they may depend on the individual's age, weight, gender, as well as everyday life. The materials assigned to the microfibrils and the crosslinks were assumed to be linear isotropic. This assumption is valid since we only focus on the elastic regime and up to 5% of deformation. Detailed properties values are shown in the tables below. ANSYS cannot accept as an input a Poisson ratio of 0.50 because the solution cannot converge. For this reason we chose to assign to cross-links a Poisson ratio of 0.48 and an Elastic Modulus of 4MPa which resembles the properties of a rubber material [31, 35]. Also, in model 2 we used a higher elastic Modulus of 6GPa to further test the contribution of the crosslinking in the stiffness of the model. The values for collagen molecules were obtained from

Sasaki and Odajima, 1996, while there was an additional model that the modulus from Silver et al. was applied to further test effect of the initial molecule's properties. The mineral has the properties that describe the mechanical behavior of Hydroxyapatite crystals (HA) with a Poisson ratio of 0.25 since it is considered a perfect linear isotropic material [30, 32, 35].

Table 5. Detailed material properties for each feature, assigned to models 1, 3 & 4.

MODELS 1, 3 & 4	Collagen	Cross-links	Mineral
Young's Modulus	2.8 GPa	4 MPa	20 GPa
Poisson Ratio	0.3	0.48	0.25

Table 6. Different detailed material properties for each feature, assigned to the models 2 & 5.

MODEL 2	Collagen	Cross-links	Mineral
Young's Modulus	2.8 GPa	6 GPa	20 GPa
Poisson Ratio	0.3	0.48	0.25

MODEL 5	Collagen	Cross-links	Mineral
Young's Modulus	7.0 GPa	4 MPa	20 GPa
Poisson Ratio	0.3	0.48	0.25

3.4 Boundary Conditions

The applied boundary conditions tried to simulate the conditions at which tensile experiments of collagen fibrils would be exposed. In the front cross sectional area the load was applied to the faces of the cylinder-molecules in parallel direction of their length axis. The model was forced to displace to 5% of its total length, thus 15 nm.

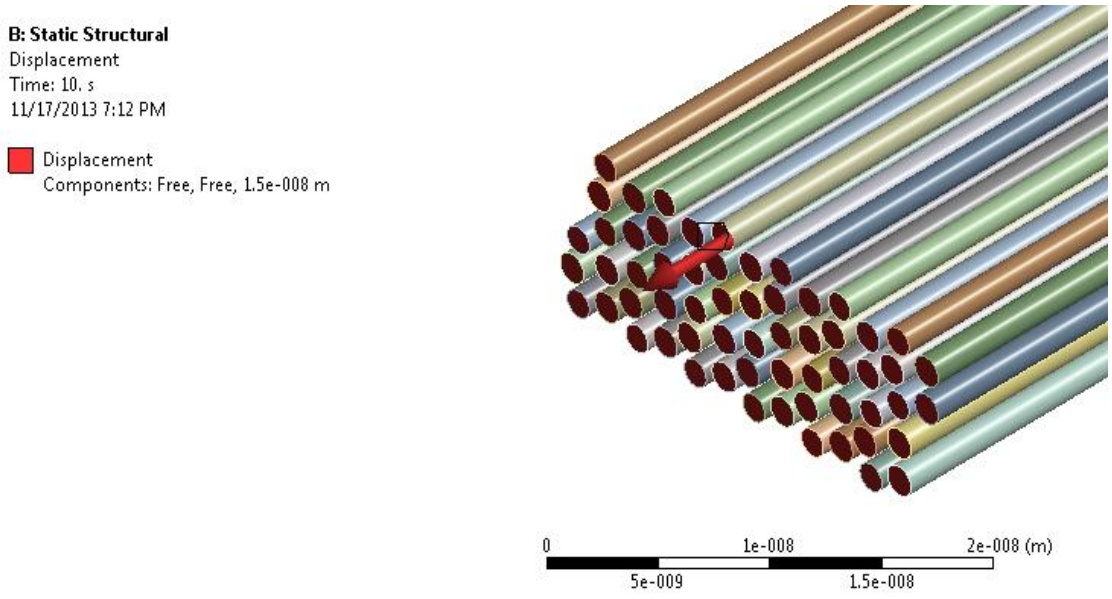

Figure 6. Boundary condition of 5% deformation at one side of the model.

There should not appear significant vertical displacements compared to the longitudinal due to the diameter/ length ratio which is almost equal to 200. The back cross sectional area had all the faces of the molecules fixed. For that reason the nodes situated at one end cross sectional part of the molecules have the following degrees of freedom constraints UZ = UX = UY = 0. Thus, this cross sectional surface is regarded to be rigidly fixed, with all translational and rotational degrees of freedom restricted. To stabilize further the complex multibody structure, a cylindrical support was applied on all the faces of the molecules, but the cylinders were left free to deform radially, UR was not fixed. This prevented the vertical and tangential displacements and allowed only the longitudinal and diametrical deformations, to avoid rigid body translations. With that assumption there was no need to apply friction coefficients on the cylindrical faces, since the molecules would not directly have surface contact. The faces of the cross-links were bonded to the cylinders and were left free without any further fixation in space [Fig. 15 & 16].

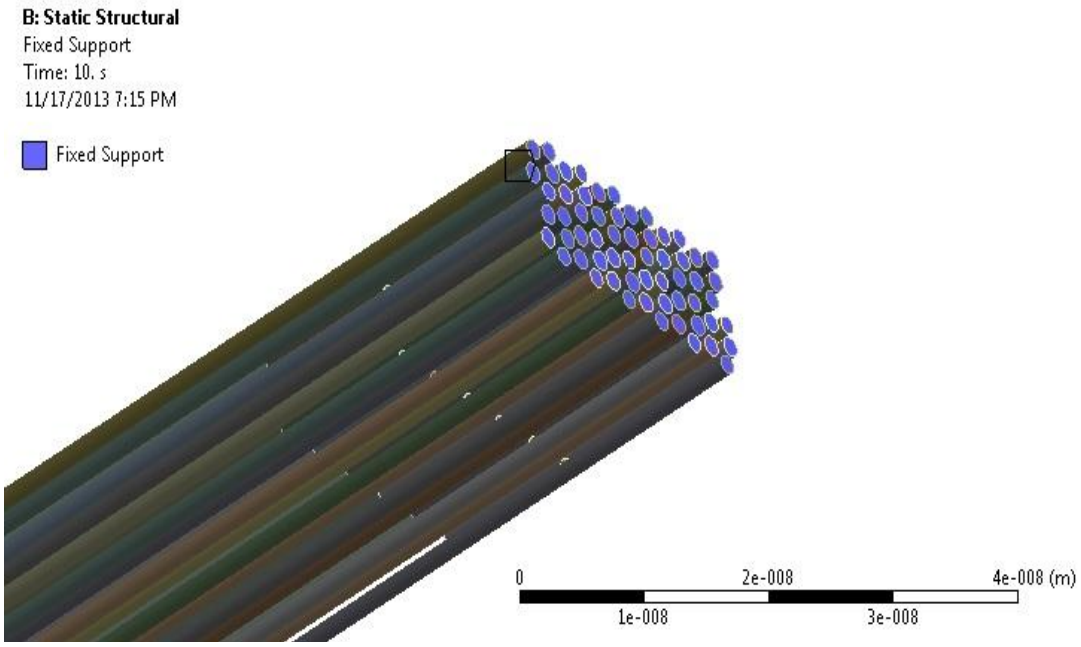

Figure 7. Fixed boundary support for the other end side of the molecules.

3.5 Parametric Testing

In this study five models were considered, while experimental data had to be obtained to refine the final models. The analyzed models were firstly the hydrated collagen model without the mineral, secondly the same with stiffer crosslinks, thirdly the hydrated and mineralized state model, fourthly the dehydrated mineralized model and finally the dehydrated mineralized model with different mechanical properties assigned for molecules. The difference between the dry and hydrated models lies in the geometry, and more particularly the diameter of the molecules which for the dry state is 1.1nm and for

the wet state close to 1.4nm. In the second, third and fourth model the mineral is found in gap regions and it forms a new cylinder that connects the in line neighboring molecules.

Table 7. All models with their detailed parameters.

MODEL	Description	Collagen Modulus	Crosslinks Modulus	Dry/Wet	Mineral
1	Wet**No**Mineral	2.8 GPa	4MPa	Wet	No
2	Wet**No**Mineral	2.8 GPa	6GPa	Wet	No
3	Wet**&**Mineral	2.8 GPa	4MPa	Wet	Yes
4	Dry**&**Mineral	2.8 GPa	4MPa	Dry	Yes
5	Dry**&**Mineral**2**	7.0 GPa	4MPa	Dry	Yes

3.6 Results

The model was forced to deform 5%. A Force probe was applied to that displacement load. With the probe force on that area the force-displacement curves were obtained. To determine material properties the force and deformation had to convert to stress-strain results from Hooke's law,

$$\sigma = \frac{F}{A}, \varepsilon = \frac{\Delta l}{lo}, \sigma = \varepsilon E.$$

Where A, is the total area of the applied force and equal to all the faces of the molecules (A_{dry} = 57nm^2, A_{wet} = 94.4nm^2), F the force probe reaction and ε the strain in percentage.

As expected the curves show a linear response up to 5% of deformation. The results for each model's static load are plotted in figures 17 and 18. The total Elastic Modulus can then be calculated from the stress-strain curve's slope [Fig. 17 & 18].

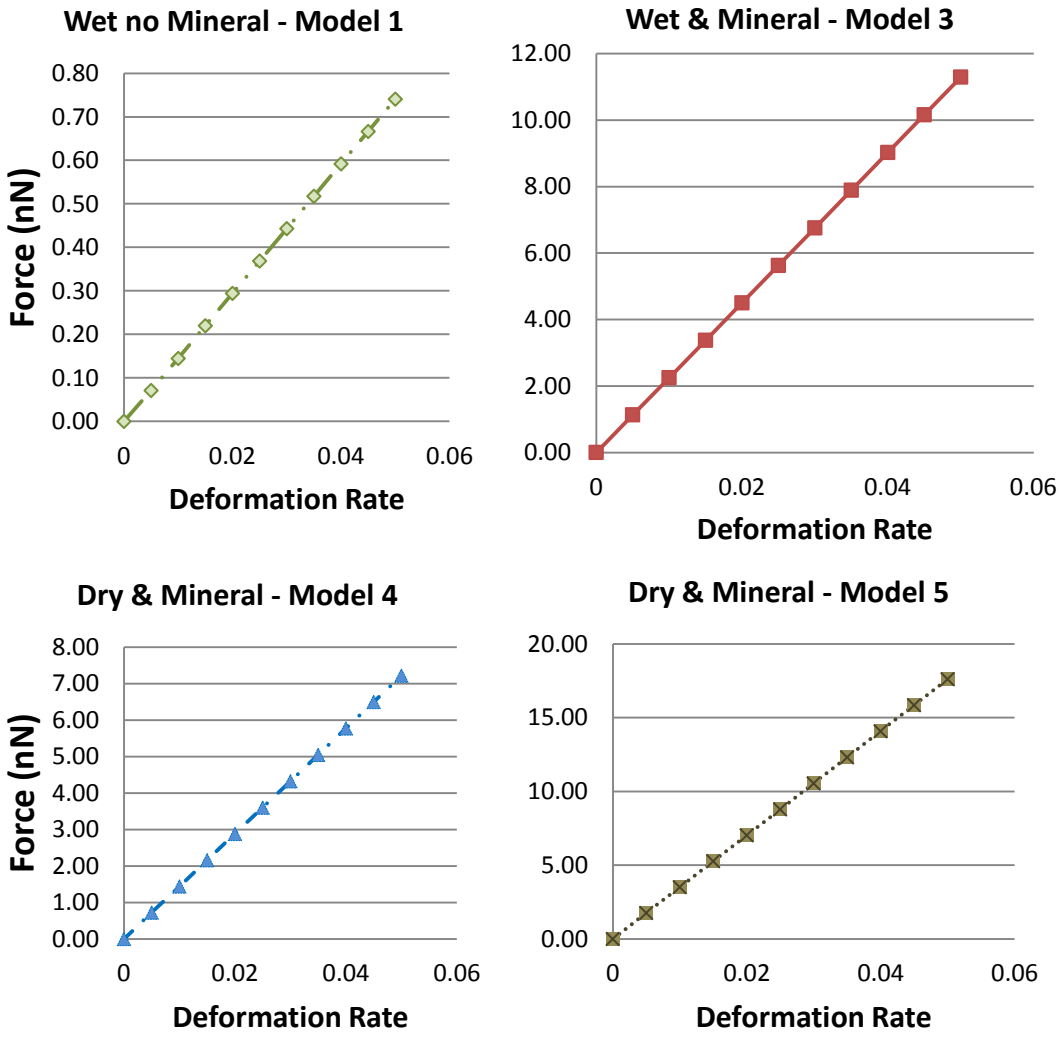

Figure 8. Force-deformation plots for each model. There is a great variation on the Force used to have the same displacement for each model.

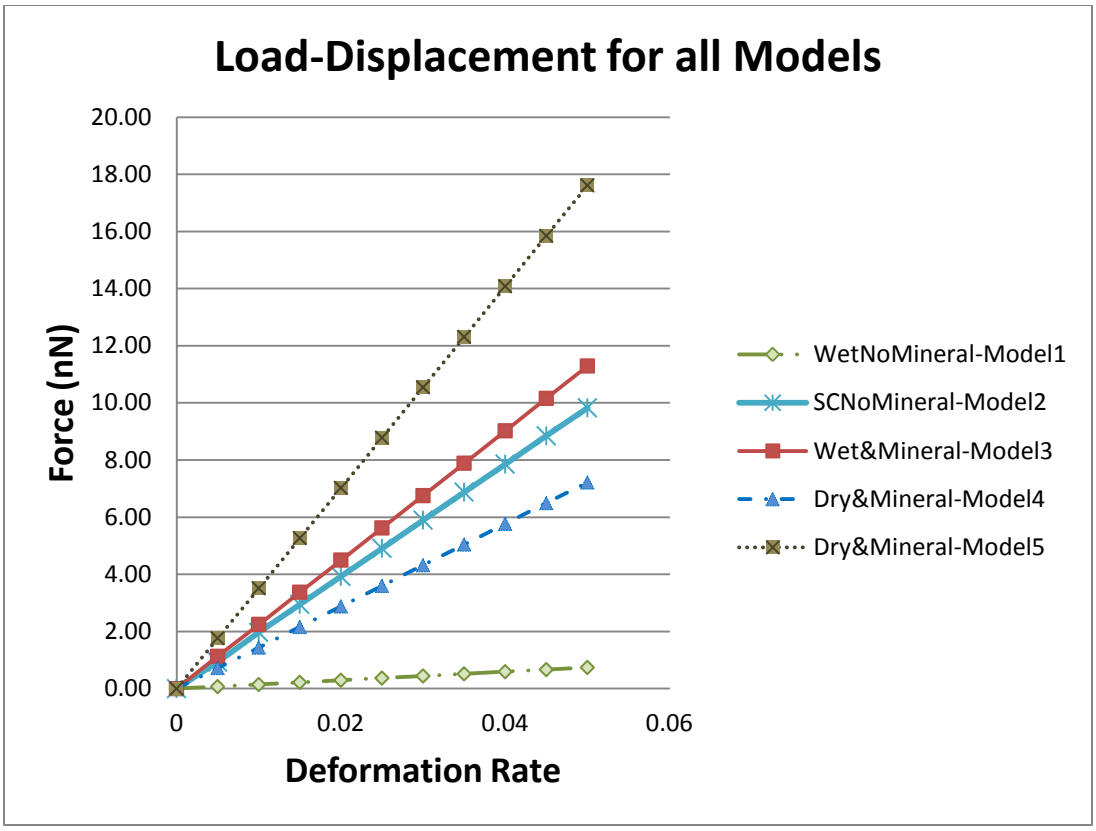

Figure 9. Overall Force-Deformation curve for all models showing higher values for both dry and mineral phase, in which the highest is as expected for the model with initial collagen modulus equal to 7GPa.

In figure 19 we can see the front view of the model and the final deformation, as well as the corresponding longitudinal displacements. As expected, the maximum displacement of 15nm occurs in the first overlapping region, mainly on the molecules that the force is applied as well as their bonded crosslinks [Fig. 19]. The same behavior was also repeated in the rest of the models.

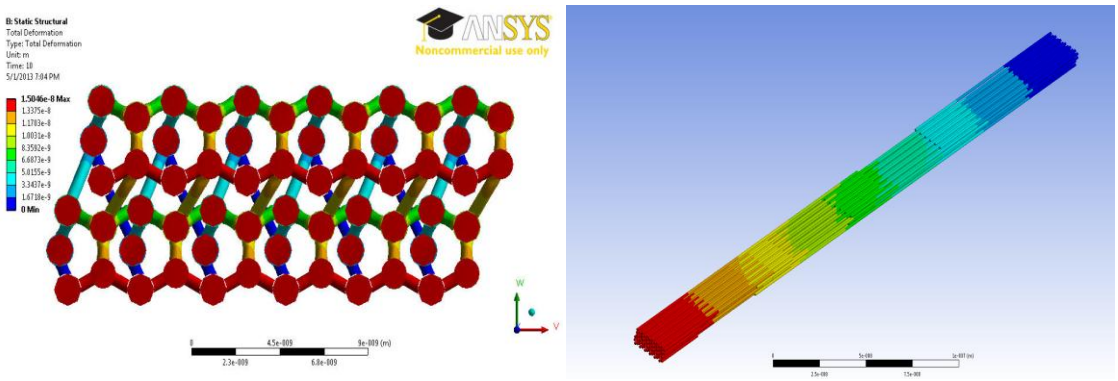

Figure 19. Projected view of final deformed shape and the longitudinal displacements on z-axis. In red is the displacement of 15nm that occurred at the frontier molecules to which the initial load was applied, along with the first region's overlapping crosslinks, again shown in red.

In the following graph the results of the wet no mineral, wet-mineral, dry-mineral, models are summarized and compared to the initial value of the collagen molecule. For the first wet no mineral model we obtain the lowest total Elastic Modulus of 0.16Gpa. This is expected since there is no mineral to fill the gap zones, thus a decrease in stiffness. For the third model of hydrated state with mineral, the elastic Modulus observed from the stress-strain curve is 2.39GPa. Compared to the molecule's initial value of 2.8GPa the overall Elastic Modulus decreased 14.64%. Finally, in the occasion of having dry microfibrils with smaller diameters, an increase in the modulus from 2.39GPa to 2.53GPa, or 5.53% is observed. This is expected since in dry state the fibrils become stiffer.

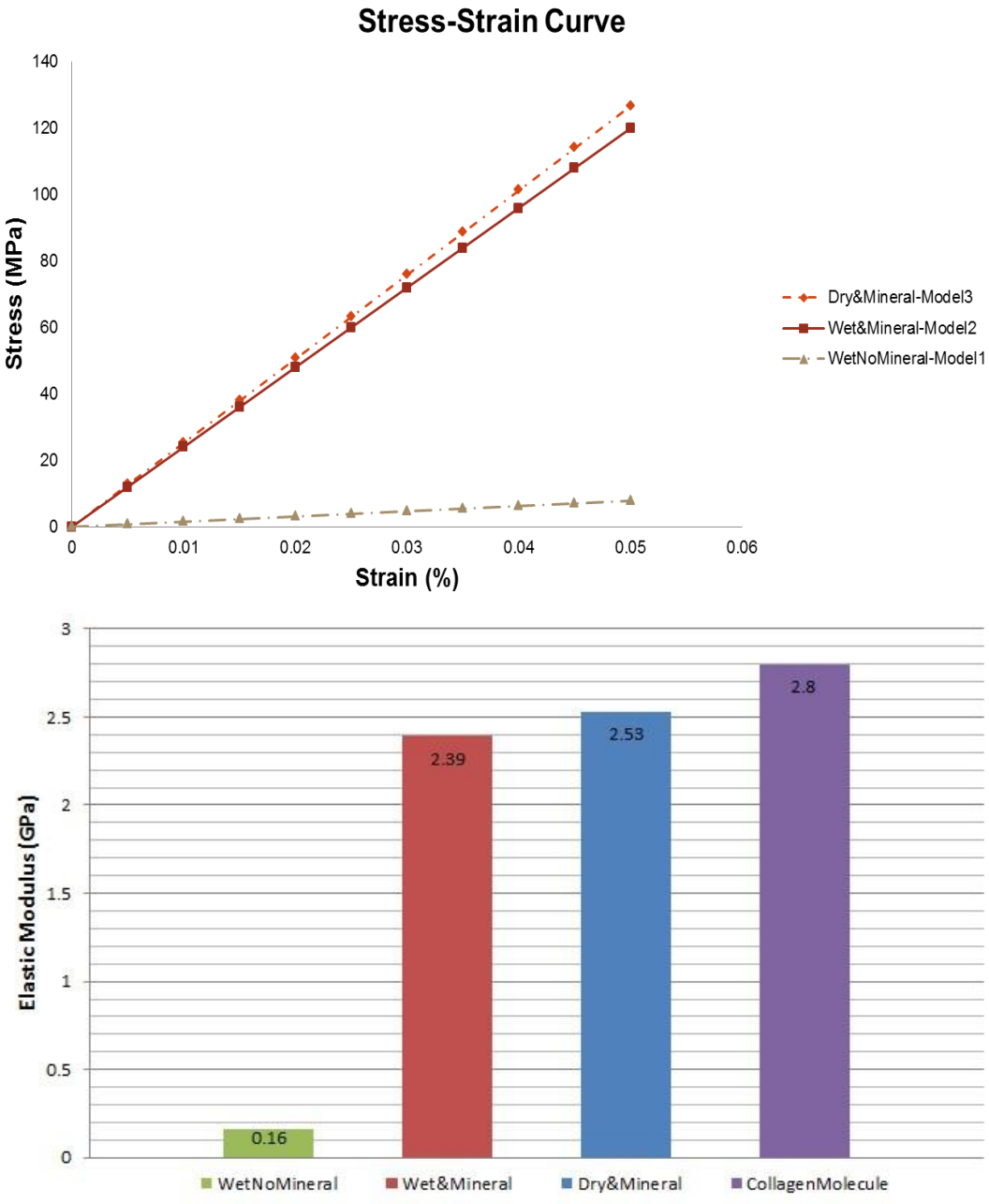

Figure 10. Stress strain curves and results for models 1, 3 & 4 compared with the initial collagen modulus.

Hydration and dehydration states are described by a molecular diameter change from 1.4nm to 1.1nm respectively. Results show that having different state of hydration does not change significantly the overall modulus. On the other hand mineralization is a parameter that has a great impact in the stiffness. We observe almost a 94% decrease of the initial modulus when there is no mineral added. Also, it is interesting to note that there is only a difference of 9.4% and 2.7% of the overall modulus from the initial collagen modulus used in models four and five, for dry and mineralized state respectively. This shows that there is not much deviation from the initial input of the molecule modulus, which means that the microfibrial mechanical response depends mainly on the stiffness of the molecules and crosslinks as well as on its inner geometry [Fig. 20 & 21]. Furthermore there is a dramatic increase from 0.16GPa to 2.39GPa when the mineral is added in the hydrated phase. Thus, the mineral in the gap region plays the most important role of enhancing the stiffness. Finally, we see in figure 21 that when we increase the initial modulus of the crosslinks from 4MPa to 6GPa there is a substantial increase in the overall modulus from 0.16GPa to 2.08GPa.

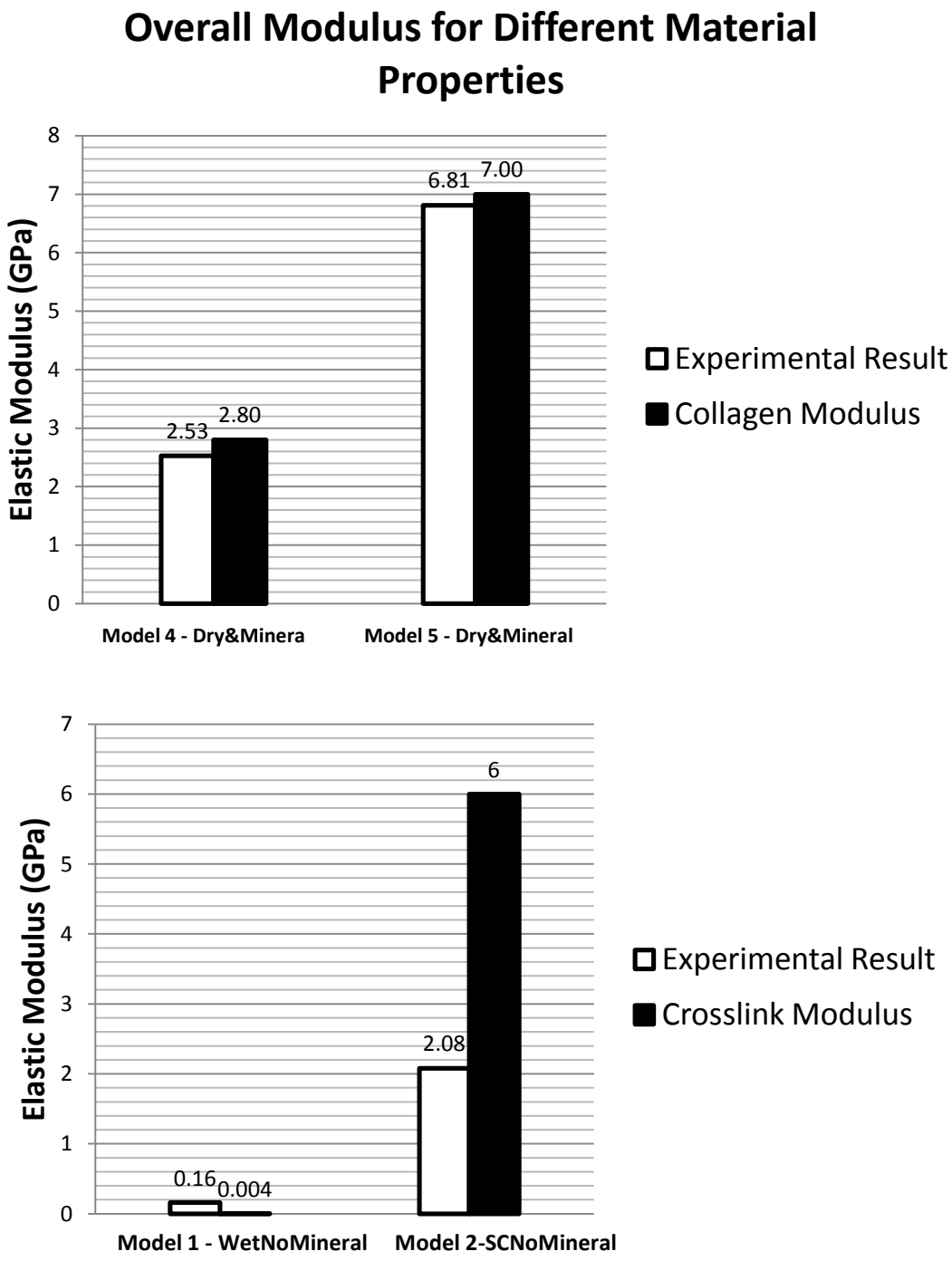

Figure 11. Total Elastic Modulus of 4-5 and 1-2 models compared to their initial input of the collagen molecule and crosslink modulus.

Von-Misses stress, or equivalent tensile stress, is used to foretell and trace the maximum yield stresses under multiaxial loads in which our model is likely to fail. This is given from the following equation,

$$\sigma_\mu = \sqrt{\frac{(\sigma_1 - \sigma_2)^2 + (\sigma_2 - \sigma_3)^2 + (\sigma_1 - \sigma_3)^2}{2}} \quad ,$$

where σ_1,σ_2,σ_3 are the principal stresses.

Maximum Von Misses stress values are summarized for all models on the following table 7 and are graphically displayed in figures 22 to 24. These results are the averaged Von Misses Stress distribution, in Pa. The location of the maximum stress can show us where each model is likely to fail if more force is applied. The actual elements and interfaces in which the maximum or minimum Von-Misses stresses appear to vary for each model. In the first scenario, where no mineral is included, the highest averaged stressed occurs in the interface of the crosslinks and the molecules on the fourth overlapping region. This is acceptable since that is the separation region of one microfibril from the other. For the rest of the models in which the mineral is added, we can see the highest Von-Misses stress distribution to be located on the Hydroxyapatite interface, where it is bonded with the molecules again at the fourth overlapping region. This can, also, be explained from the fact that the mineral is the feature with the stiffest mechanical behavior, and is almost the same scale of the stiffness of molecules. The maximum stress developed surpasses 0.39GPa for the third one.

Table 8. Summarized results for total modulus and Von-Misses stress.

MODEL	Description	Elastic modulus	Max Von-Misses Stress	Max Von-Misses Element	Min Von-Mises Element
1	Wet**No**Mineral	0.16GPa	0.24GPa	Crosslink4	Molecule1
3	Wet**&**Mineral	2.39GPa	0.51GPa	HA4	Crosslink8
4	Dry**&**Mineral	2.53GPa	0.39GPa	HA4	Crosslink5

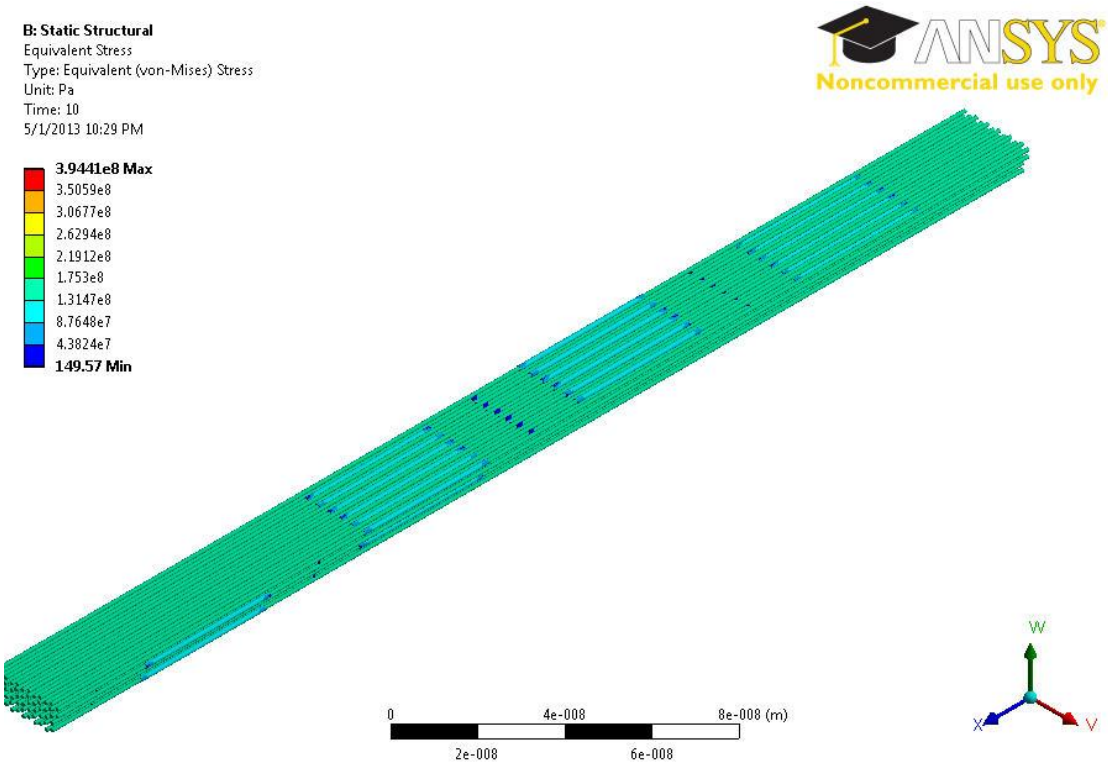

Figure 12. Equivalent Von-Misses stress distribution for Dry & Mineral State, Model 4.

The equivalent von Misses stress occurred mainly at the interface of the molecule-crosslink or molecule-hydroxyapatite, when mineral was added. The most interesting conclusion is that for models 3 and 4 the maximum stress developed on the same mineral – molecule interface in the fourth overlapping region. Additionally, in model 1 when there was no mineral, the maximum stress distribution was observed again in the fourth region but this time on the crosslink-molecule bonded interface. Also, a higher modulus

of the collagen microfibrils leads to an increased stiffness of the fifth model along the horizontal axis.

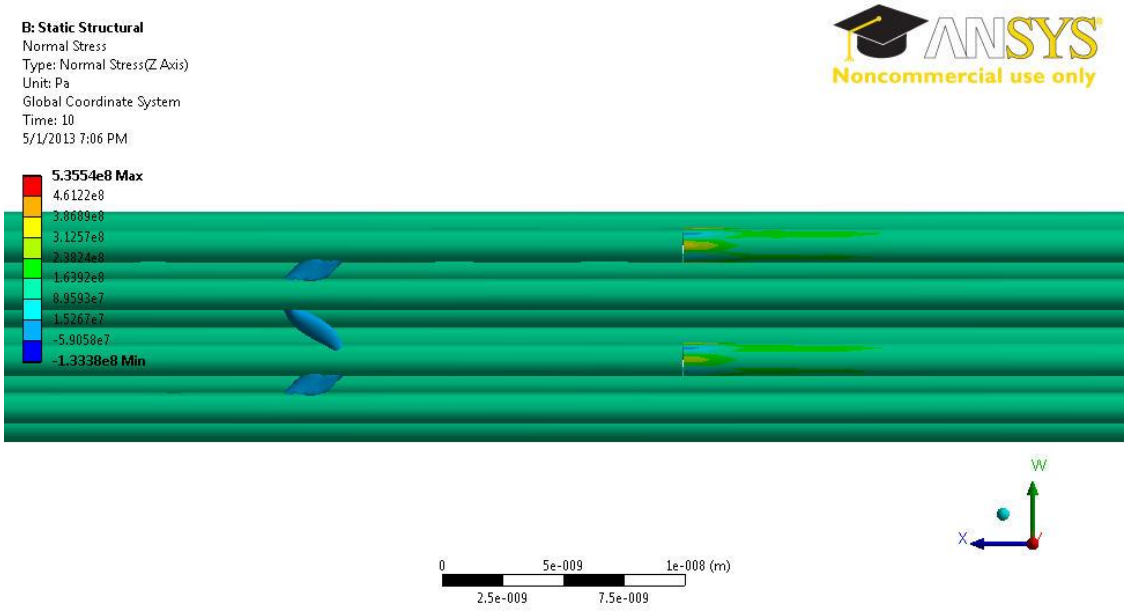

Figure 13. Equivalent Von-Misses stress distribution for Dry & Mineral State, Model 5.

It is interesting to note that some of the crosslinks in all regions appear to be almost stress free for all five models, as shown in detail on Appendix, especially in the first and fifth overlapping region [Fig. 27-35]. Not all crosslinks contribute equally to the load transfer. This depends on their geometry and packing. Even crosslinks that appear in the same overlapping regions do not have equal Von-Misses stress distributions, with the longest ones being more stress free [Fig. 23 & 24, Appendix]. This suggests that they do not contribute much in the axial tensions resistance, while they could potentially have an impact if the load was distributed in different directions.

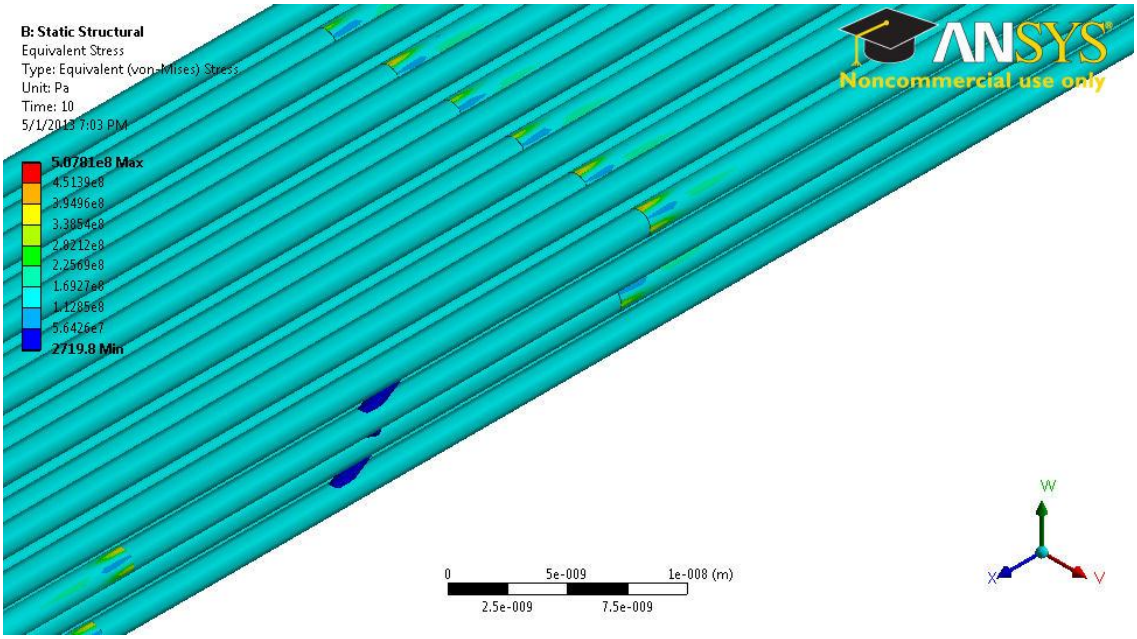

Figure 14. Equivalent Von-Misses stress distribution for Wet & Mineral State, Model 3.

The analysis for the 1, 3 and 4 models agrees qualitatively with available experimental data, and results are close to the reality. This collagenous network enhances the tensile strength, while the mineral provides the highest rigidity. In the study of Hambli and Barkaoui [22], the authors report a Young's modulus of 1.9GPa for dry state and 0.26GPa for hydrated state, thus their elastic modulus is highly influenced by the state. In our study the state did not have such a big influence as we report a Young's modulus of 2.59GPa for dry and 2.39GPa for wet state, while the main difference occurred in the E=0.16GPa for no mineralization. Their stress-strain curves in tension and compression were, also, found to be linear. Finally, while their crosslinks were placed at random, our

model demonstrates specific and increased in number crosslinking staggering as described in literature.

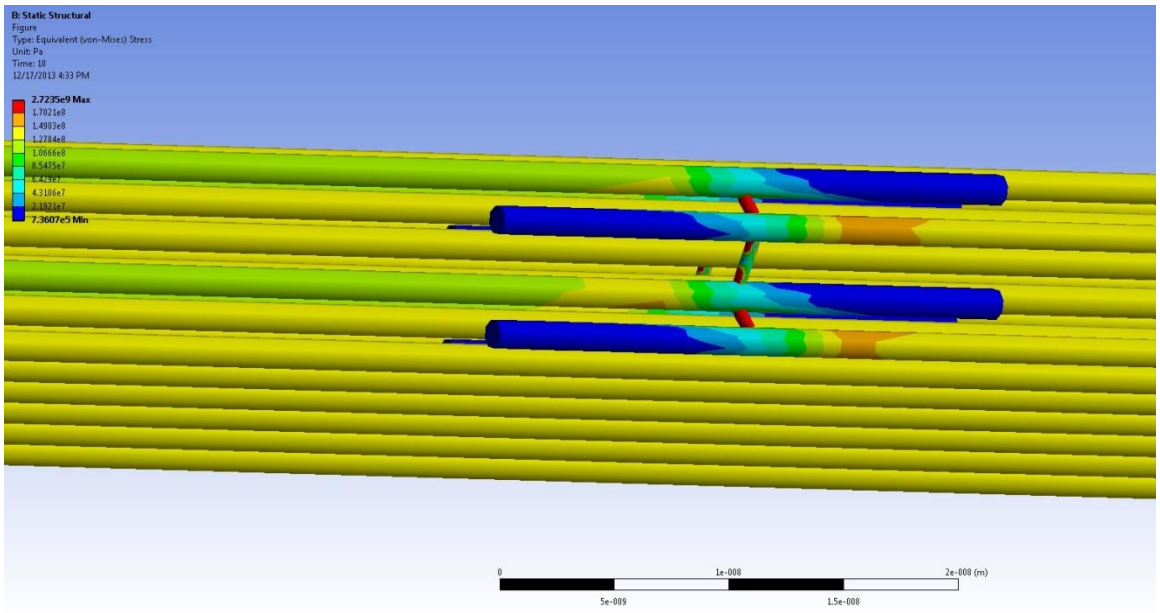

Figure 25. Equivalent Von-Misses stress distribution for Wet & Mineral State, Model 2.

Finally, in Figure 25 we can see the Von Misses distribution of the fourth overlapping region for model 2, in which we increased the stiffness of the crosslinks from 4MPa to 6GPa [Appendix, Fig. 36-37]. The overall model became stiffer and the maximum stress was equal to 2.72GPa shown in red. Thus, it is clear that by increasing the modulus of the crosslinks we can achieve a stiffer model.

CHAPTER 4

CONCLUSIONS

4. CONCLUSIONS

Five detailed numerical models of tendon's microfibrils were studied in this thesis. The main focus was on the linear part beyond the toe-region that was associated with the loading of the straight microfibrils. In previous studies there are reported large variations in the magnitude of the elastic modulus in this region. Some studies report values in the magnitude of MPa while others report values of GPa [Table 1]. Our results are highly comparable to these previous studies. In the study of Silver et al, for mineralized turkey tendons, the authors report that the Elastic Modulus is proportional to the mineral content in collagen fibrils [19]. They estimated the modulus to vary from 5.48GPa to 7.22GPa when the mineral weight fraction was more than 0.215. This is highly comparable to our study since in Model 5 we report an overall modulus of 6.81GPa with an 18% mineral content.

The advantage of the five models that were used was the accurate modeling of both the fibrils shape and their structure from their known physiological parameters as well as of the potential behavior of their materials. This work was completed with respect to the experimental data available from previous well-esteemed studies. The requirement to investigate various models originates from the issue that both the accurate behavior and geometry of the fibril are not exactly defined in hydration, dehydration and mineralization.

Moreover, the complexity of the models is enhanced by the fact that the models must be adaptive and computationally time efficient. All models were subjected to static load. The complexity of the structure of collagen in different levels of hierarchy obstructs comprehension of its mechanical properties and behavior. The uniqueness of this analysis is the approach of understanding tendon's mechanical behavior in this scale.

Our conclusion is that the overall model response depends substantially on mineralization and hydration state. The results reported confirm the functionality of this 3D finite element model in this scale for static loading and justify the results found by previous empirical and experimental studies.

Our efforts also prove that the manner in which the molecules of collagen are linked can have a profound effect on the strength, stiffness and vulnerability of the tissue. When we increased the modulus of the crosslinks we observed a substantial increase also in the overall model's stiffness from 0.16GPa to 2.08GPa. Moreover, increased number of crosslinks shows dramatic increase on the overall stiffness. This is evident from Hambli and Barkaoui's FEA study, in which they report a 0.26GPa for wet and 1.9GPa for dry state compared to the 2.39GPa and 2.53GPa respectively from this study. The length of the model, boundary conditions and molecule's initial material properties were the same. However, their model was using only 5-10 crosslinks while in our work there are 97 specifically positioned crosslinks, thus increase on the molecule bodies in cross-section.

The overall model was as expected less stiff than the stiffness of its components, with collagen being the stiffest one. Therefore, reports that show values of fibril modulus being lower than the tendon modulus should be questionable. Despite the fact that the macroscopic tissue function is of high importance, the multi-level approach focusing at the lower levels of hierarchy would be helpful to understand the overall tissue function and physiology.

The assumptions we made are also used in other computational studies in order to have less computational time and to eliminate non-convergence. Moreover, assumptions of the linear isotropic materials that were assigned to each feature, do not contribute much since we are focusing on the elastic regime of the initial 5% total deformation. This, also, compensates for the mechanical behavior and properties of each component that either are not defined clearly in literature or lay under conflict opinions. The main contribution of the present work is eventually to be able to represent all the levels of hierarchy in detail and thus have an ultimate model of the tendon that describes its function. This requires appropriate knowledge of all the physiological parameters involved as well as the structure. However, this cannot be achieved without the computational CPU capabilities that still lack nowadays.

For future work the model can increase its abilities by adding friction coefficients among the molecules and eliminating the restriction to move tangentially. Also, with the appropriate Finite Element software the model would be able to have more elements, thus increase in size, crosslinks and potentially escalate to a higher level of hierarchy.

Furthermore, a more dynamic structure could be set to measure the model's viscoelasticity with stress-relaxation tests without necessarily including the 5% limitation of total deformation.

Finally, more parameters should be considered in order to simulate models that would represent individuals, according to their age, gender and everyday habits. Although, this is still beyond current available means, more improvements can be suggested such as the accurate simulation of the collagen fibrils and fascicles beginning from the very initial level, with the help of quantitative computer tomography scans. Moreover, each physiological parameter should be considered as a different feature or element with its own set of mechanical properties. The geometry should also include random collagen Y-branches since these have been reported in literature. If after all these improvements, the time required for the analysis does not increase substantially, then these additions would benefit the analysis to remain flexible and in parallel with the experimental results. This field of finite element modeling is gradually improving in biomechanics and biomedicine since the ultimate goal is to avoid experimental destructive tests or animal testing.

APPENDIX

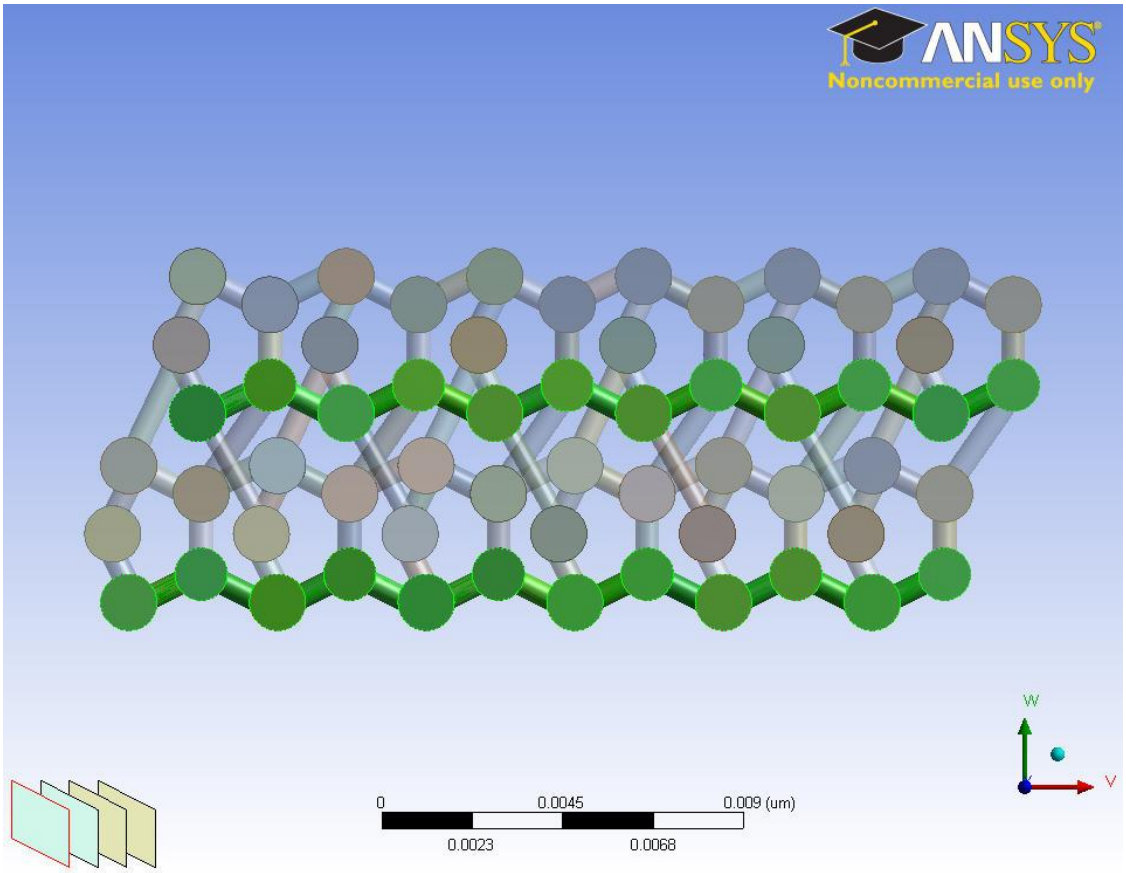

Figure 26. Crosslinking of 1 to 5 staggered molecules in the first overlapping region.

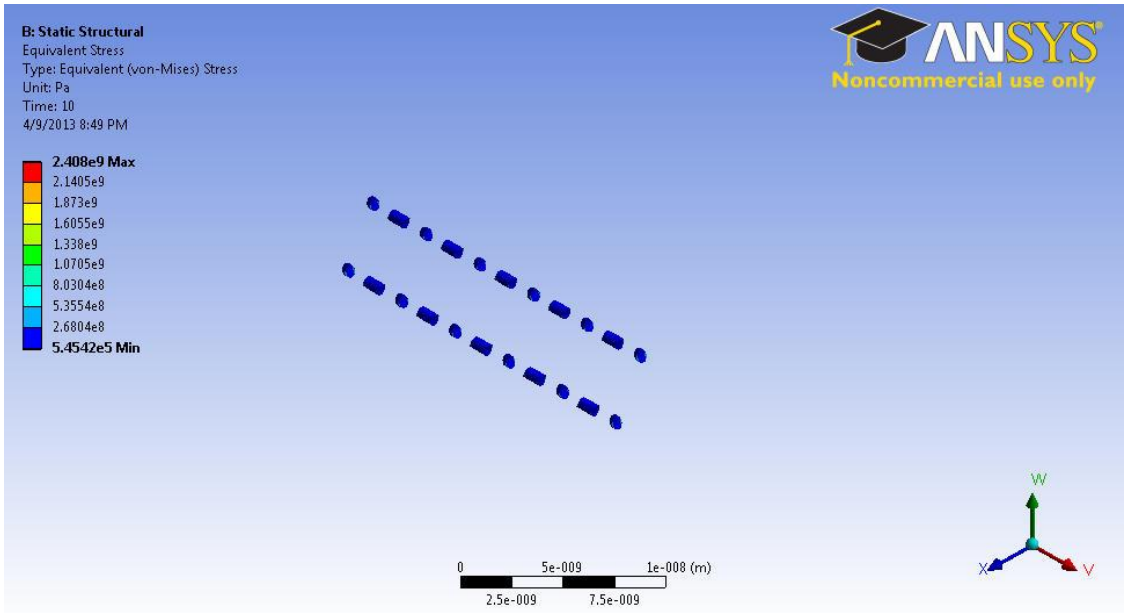

Figure 27. Von-Misses stress of 1 to 5 staggered molecules in the first overlapping region.

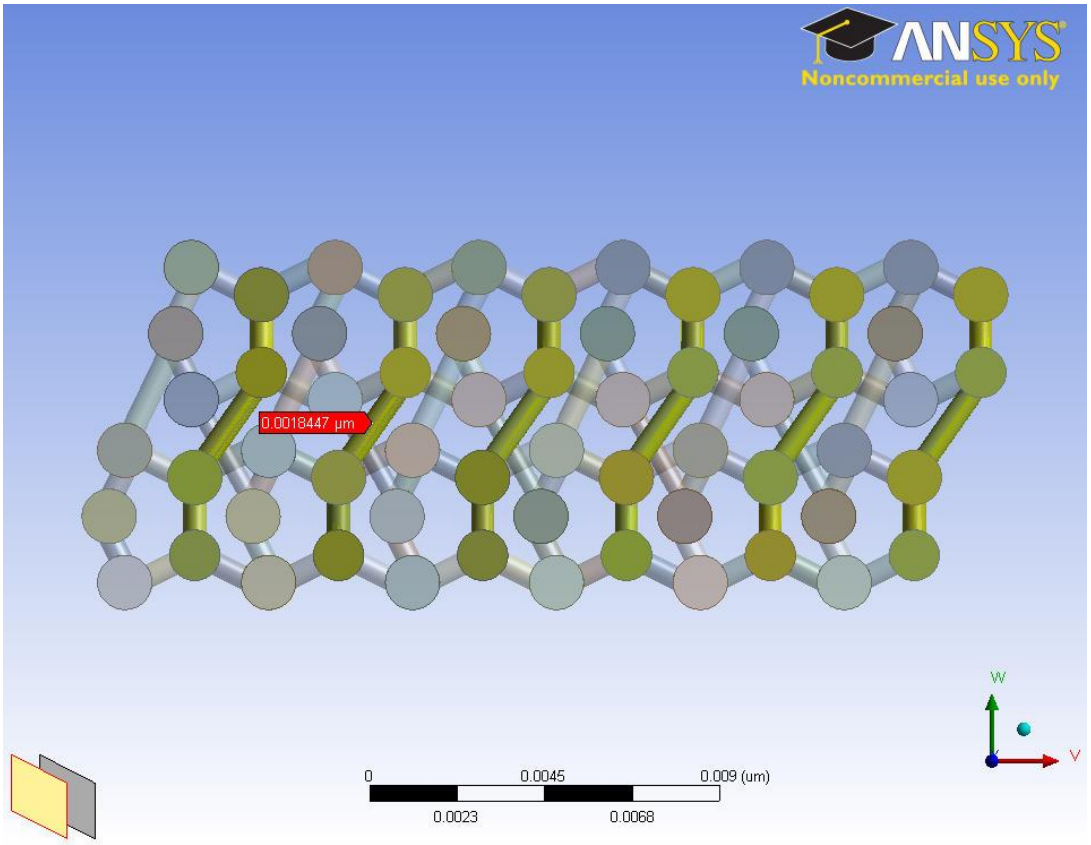

Figure 28. Crosslinking of 1 to 5 staggered molecules in the second overlapping region.

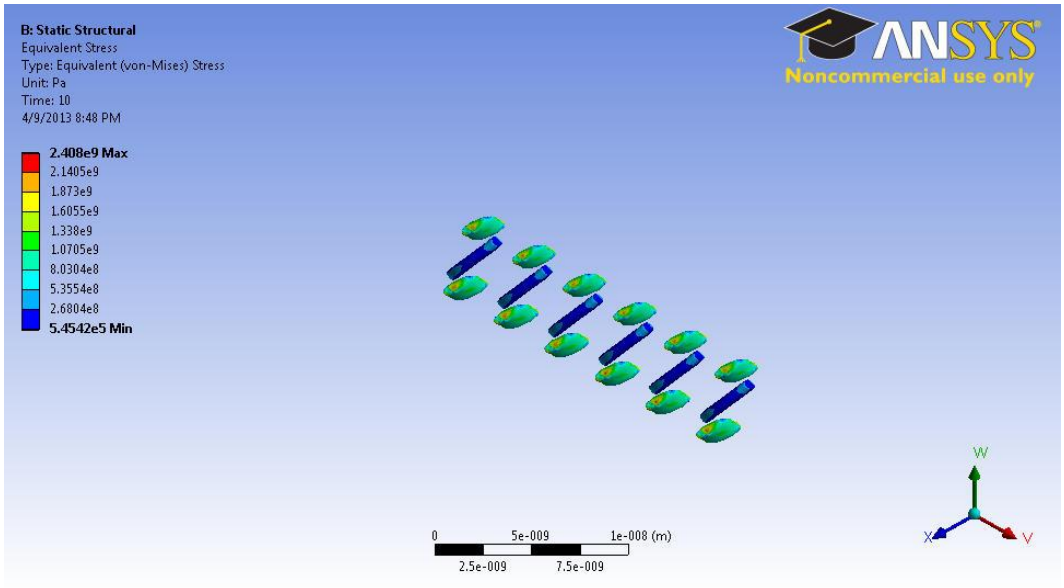

Figure 29.Von-Misses stress of 1 to 5 staggered molecules in the second overlapping region.

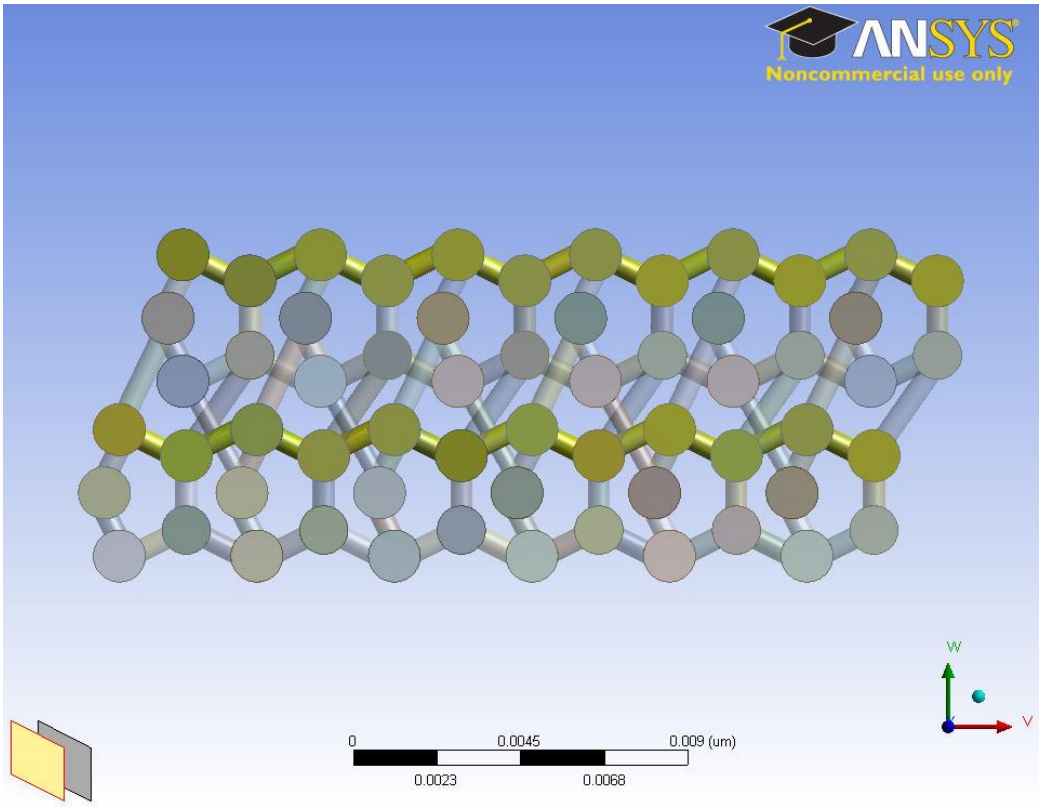

Figure 30. Crosslinking of 1 to 5 staggered molecules in the third overlapping region.

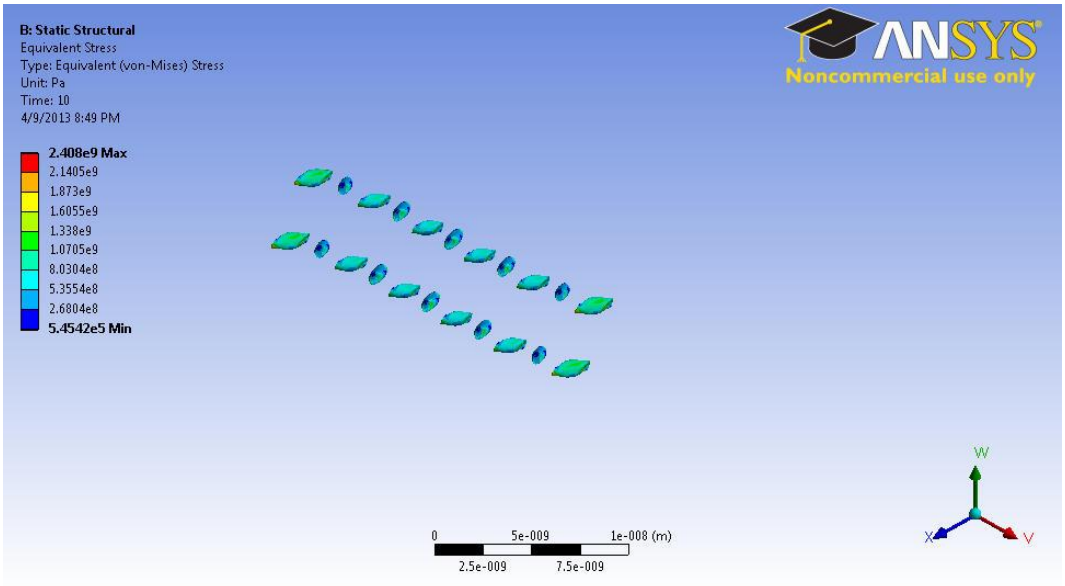

Figure 31.Von-Misses stress of 1 to 5 staggered molecules in the third overlapping region.

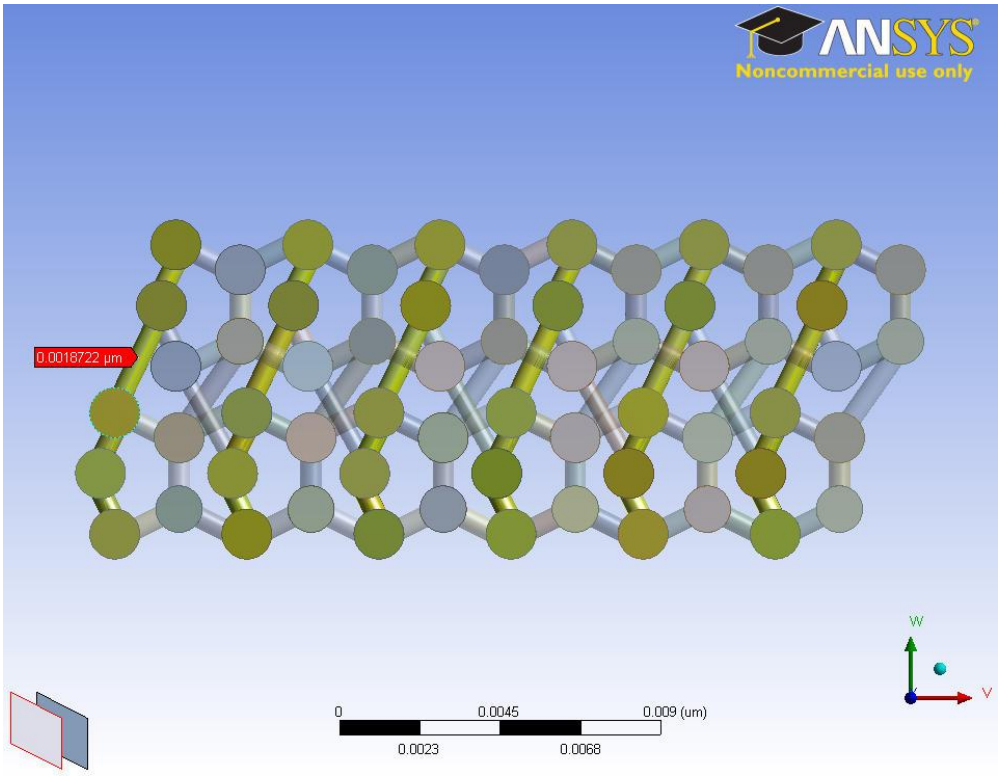

Figure 32. Crosslinking of 1 to 5 staggered molecules in the fourth overlapping region.

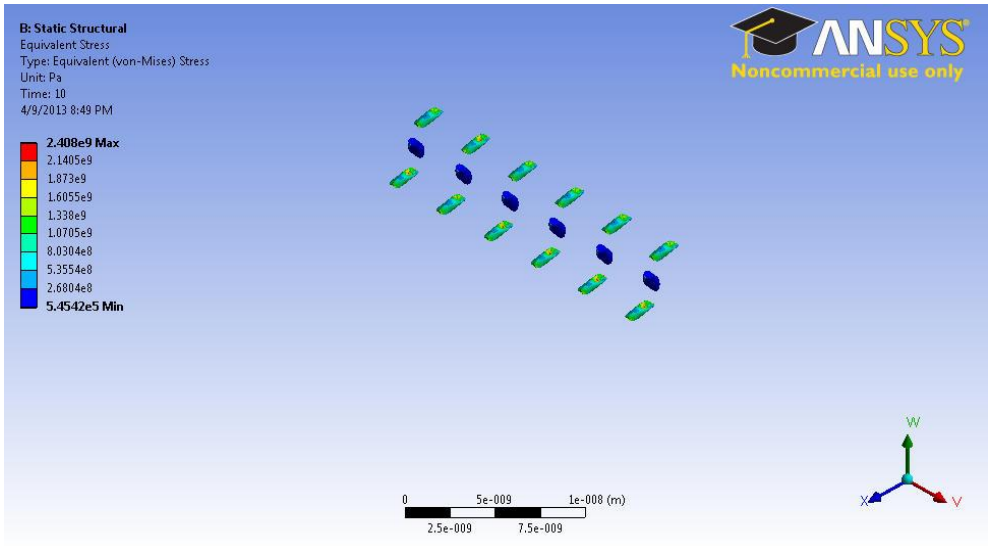

Figure 33.Von-Misses stress of 1 to 5 staggered molecules in the fourth overlapping region.

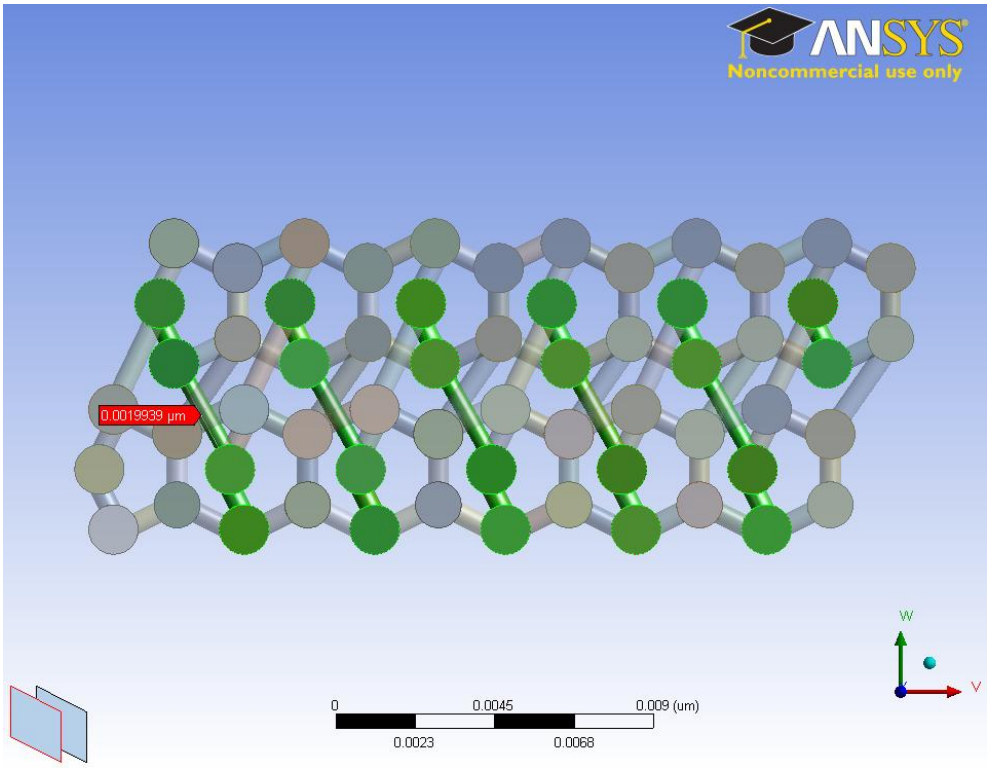

Figure 34.Crosslinking of 1 to 5 staggered molecules in the fifth overlapping region.

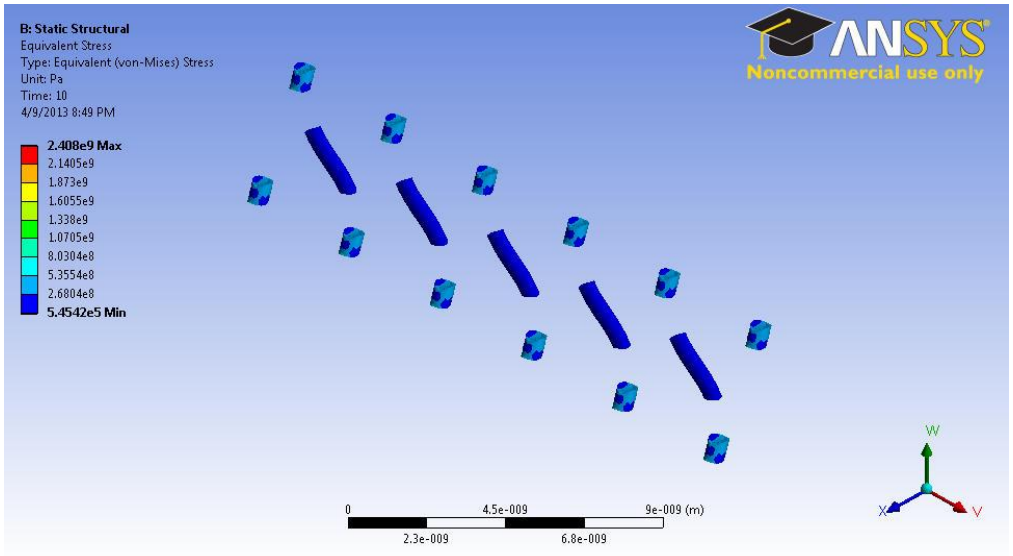

Figure 35.Von-Misses stress of 1 to 5 staggered molecules in the fifth overlapping region.

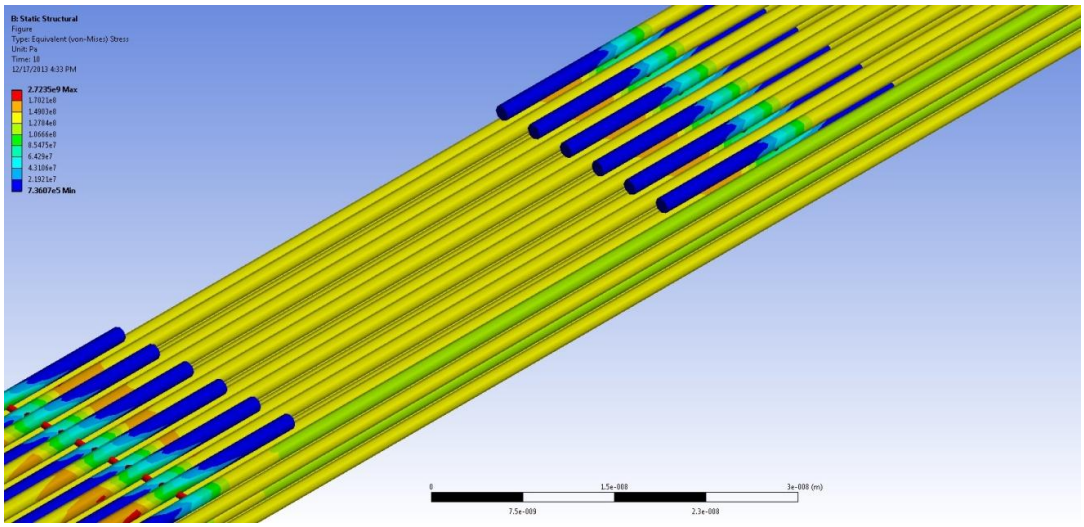

Figure 36.Von-Misses stress distribution in the third and fourth overlapping region for model 2.

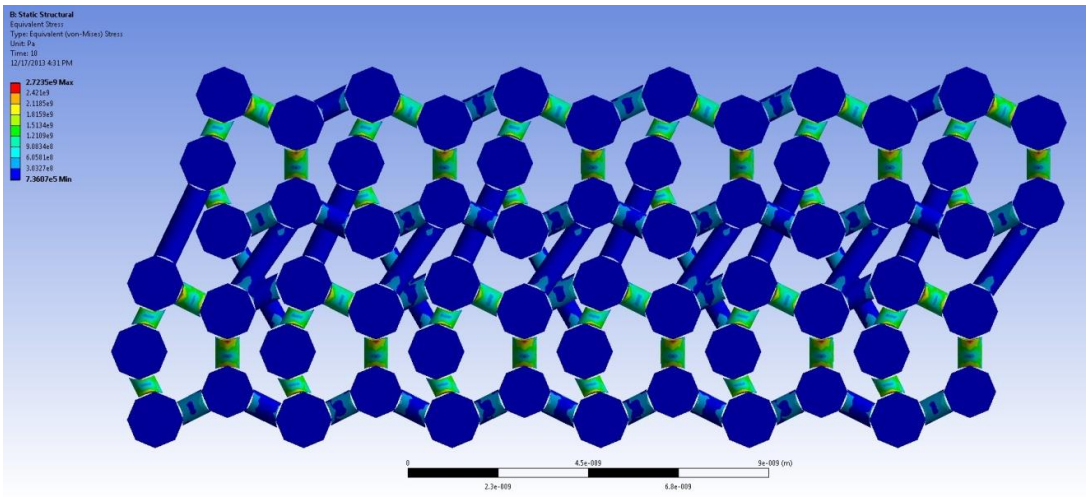

Figure 37.Overall projected Von-Misses stress for model 2 showing stress distribution on crosslinks.

BIBLIOGRAPHY

1. Orgel J., Irving T., Miller A., and Wess T., Microfibrillar structure of type I collagen in situ, PNAS, Vol. 103, 9001-9005, 2006.
2. Sasaki N. and Odajima S., Elongation Mechanism of Collagen Fibrils and Force-Strain Relations of Tendon at Each Level of Structural Hierarchy, J. Biomechanics, Vol.29, 1131-1136, 1996.
3. Sasaki N. and Odajima S., 1996, Stress Strain Curve and Young's Modulus of a Collagen Molecule as Determined by the X-ray Diffraction Technique, J. Biomechanics, Vol.29, 655-658, 1996.
4. Gautieri A., Pate M., Vesentini S., Redaelli A., Buehler M., Hydration and Distance Dependence of Intermolecular Shearing Between Collagen Molecules in a Model Microfibril, J.Biomechanics, Vol. 45, 2079-2083, 2012.
5. Fratzl P., Fratzl-Zelman N., Klaushofer K., Collagen Packing and Mineralization, J. Biophysics, Vol. 63, 260-266, 1993.
6. Puxkandl R., Zizak I., Pari O., Kecke J., Tesch W., Bernstorff S., Viscoelastic Properties of Collagen: Synchrotron Radiation Investigations and Structural Model, Phil. Trans. Royla Society London, Vol. 357, 191-197, 2002.
7. Franchi M., Trirè A., Quaranta M., Orsini E., and Ottani V., Collagen Structure of Tendon Relates to Function, Scientific World Journal, Vol. 7, 404-20, 2007.
8. Lorenzo A.C., Caffarena E.R., Elastic properties, Young's modulus determination and structural stability of the tropocollagen molecule: a computational study by steered molecular dynamics, Journal of Biomechanics, Vol. 38, 1527–1533, 2005.
9. Shen Z., Kahn H., Ballarini R., and Eppell S., Viscoelastic properties of isolated collagen fibrils, Biophysical Journal, Vol. 100, 3008–3015, 2011.
10. Starborg T, Lu Y, Huffman A, Holmes D. F, Kadler K. E., Electron microscope 3D reconstruction of branched collagen fibrils in vivo, Scand J Med Sci Sports, Vol. 19(4), 547-52, 2009.
11. Zhang D., Chippada U., and Jordan K., Effect of the structural water on the mechanical properties of collagen-like microfibrils: A molecular dynamics study, Annals of Biomedical Engineering, Vol. 35, 1216–1230, 2007.
12. Bailey A.J., Light, N.D., and Atkins E.D.T., Chemical cross-linking restrictions on models for the molecular organization of the collagen fibre, Nature, Vol. 288, 408 – 410, 1980.
13. Gautieri A., Vesentini S., Redaelli A., Buehler M., Viscoelastic properties of model segments of collagen molecules, Matrix Biology, Vol. 31, 141–149, 2012.
14. Doillon C., Dunn M., Bender E., Silver F., Collagen Fiber Formation in Repair Tissue: Development of Strength and Toughness, Collagen Res., Vol. 5, p 481-492, 1985.
15. Silver F.H., Christiansen D., Snowhill P., Chen Y., Transition from Viscous to Elastic-Based Dependency of Mechanical Properties of Self-Assembled Type I Collagen Fibers, Journal of Applied Polymer Science, Vol 79, 134-142, 2001.

16. Silver F.H., Christiansen D., Snowhill P., Chen Y., Landis W., The Role of Mineral in the Storage of Elastic Energy in Turkey Tendons, Biomacromolecules, Vol. 1, 180-185, 2000.
17. Silver F.H., Christiansen D., Snowhill P., Chen Y., Role of Storage on Changes in the Mechanical Properties of Tendon and Self –Assembled Collagen Fibers, Connective Tissue Research, Vol. 41(2), 155-164, 2000.
18. Christiansen D., Huang E., Silver F.H., Assembly of type I collagen: fusion of fibrils subunits and the influence of fibril diameter on mechanical properties, Matrix Biology, Vol. 19, 409-420, 2000.
19. Silver F.H., Freeman J., Horvath I., Landis W., Molecular Basis for Elastic Energy Storage in Mineralized Tendon, Biomacromolecules, Vol. 2, 750-756, 2001.
20. Seehra G., and Silver F.H., Viscoelastic properties of acid- and alkaline-treated human dermis: a correlation between total surface charge and elastic modulus, Skin Research and Technology, Vol. 12, 190-198, 2006.
21. Silver F.H., A Molecular Model for Linear and Lateral Growth of Type I Collagen Fibrils, Collagen Rel. Res. Vol. 2, 219-229, 1982.
22. Hambli R., Barkaoui A., Physically based 3D finite element model of a single mineralized collagen microfibril, Journal of Theoretical Biology, Vol. 301, 28-41, 2012.
23. Silver F.H., Freeman J., Seehra G., Collagen self-assembly and the development of tendon mechanical properties, Journal of Biomechanics, Vol. 23, 1529-1553, 2003.
24. Silver F.H., and Landis W., Deposition of Apatite in Mineralizing Vertebrate Extracellular Matrices: A Model of Possible Nucleation sites on Type I Collagen, Connective Tissue Research, 1-13, 2011.
25. Svensson R., Tendon Force Transmission at the Nanoscale, Institute of Sports Medicine Copenhagen, PhD Thesis, 2012.
26. Satraki M., and Kourkoulis S. K., A Comparative Study of the Mechanical Response of Various Numerical Models of the Human Lumbar Intervertebral Disc, National Technical University of Athens, Greece, 2008.
27. Roylance D., Finite Element Analysis, Massachusetts Institute of Technology, 2001.
28. Lee H., Finite Element Simulations with Ansys Workbench 13, Paperback, Schroff Development Corp, 2011.
29. Arroyo M. and Belytschko T., Finite element methods for the non-linear mechanics of crystalline sheets and nanotubes, Int. J. Numer. Meth. Engng, Vol. 59, 419–456, 2004.
30. ASTM, F394-78. Standard test method for biaxial flexure strength modulus of rupture of ceramic substrates, 424 – 28, 1991.
31. South J.T., Mechanical Properties and Durability of Natural Rubber Compounds and Composites, Dissertation, Blacksburg Virginia, 2001.
32. Pinchuk N., Kuda O., Ivanchenko L., Lazorenko V., Leonowicz M., Szutkowska M., Processing and characterization of glass reinforced biogenic hydroxyapatite composites with ferromagnetic additives, Processing and Application of Ceramics,Vol. 2, 45–51, 2008.

33. Cui F. Z., Li Y., Ge J., Self-assembly of mineralized collagen composites, Materials Science and Engineering, Vol. 57, 1–27, 2007.
34. Holmes D.F., and Kadler K.E., The 10+4 microfibril structure of thin cartilage fibrils, Proceedings of National Academic Sciences, PNAS, 2006.
35. Silver F.H., Mechanosensing and Mechanochemical Transduction in Extracellular Matrix, Springer, 2006.
36. Hodge, A.J., and Petruska J.A., Recent studies with electron microscope on ordered aggregates of the tropocollagen macromolecule. In aspects of Protein Structure, G.N. Ramachandran, pp. 289-300, New York: Academic press, 1963.
37. Landis W., Silver F.H. and Freeman J., Collagen as a scaffold for biomimetic mineralization of vertebrate tissues, J. Mater. Chem., Vol. 16, 1495–1503, 2006.